Interaction Notes
Note 112

May 1972

Numerical Results of the Singularity Expansion Method as Applied to a Plane Wave Incident on a Perfectly Conducting Sphere

Joe P. Martinez
Zoe Lynda Pine
F. M. Tesche

The Dikewood Corporation
Albuquerque, New Mexico

singularity expansion method (SEM), plane waves, conduction

Abstract

The singularity expansion method is applied to the problem of a plane wave incident on a perfectly conducting sphere. Surface current and charge density responses are calculated for a delta function in the frequency domain and step function in the time domain. The effect of adding individual poles to the expansion is noted. Calculations performed by the more conventional frequency domain-inverse Fourier transform solutions are included for comparison.

TABLE OF CONTENTS

In a recent note, a new approach for the analysis of EMP problems was described by Baum.[1] The technique, referred to as the Singularity Expansion Method, describes the scattering properties of an obstacle in terms of poles of the response function which occur in the complex frequency plane associated with the Laplace transform of the time domain function.

Associated with each pole is a natural mode and a coupling vector which are independent of the type of excitation. The coupling vector and the incident field define a coupling coefficient which does depend on such factors as angle of incidence and polarization of the incident field. With the pole locations, the natural modes and the coupling coefficients, the delta function time response of the scatterer may be rapidly computed. More general waveforms may then be treated by convolution techniques.

In addition to being able to easily compute the time domain response of a scatterer, this method provides a means to characterize the complete electromagnetic behavior of the obstacle by a few numbers. Once the natural frequencies, modes and coupling coefficients are known, a wide variety of scattering problems can be rapidly determined without having to re-solve the boundary value problem. From this standpoint, the Singularity Expansion Method is clearly more desirable than the conventional frequency domain or direct time domain solutions.

For a general body, it is difficult to determine the locations of the natural frequencies. A numerical search procedure is usually employed. As pointed out by Baum, the special case of a spherical obstacle can be treated in this manner, and the natural resonances found in terms of the zeros of certain spherical Hankel functions. Stratton[2] briefly considers this question.

Other investigators have treated various aspects of the Singularity Expansion Method. Marin and Latham[3] have looked at the analytical

properties of the scattered field by a perfectly conducting, finite body, using the H-field integral equation. That a finite, perfectly conducting body has only poles in the complex s plane has been verified. Lee and Leung[4] have developed explicit formulas for the natural resonance frequencies of a thin cylinder, using a Wiener-Hopf technique. Their results are valid, however, only for very thin wires. More general numerical results for the thin-wire scatterer have been obtained by Tesche,[5] where the pole location, natural modes, and time behavior of charge and currents are computed using the E-field integral equation. The results in that note as obtained by the singularity approach are shown to agree very well with those of the conventional frequency domain method.

In this note, some numerical results for the case of scattering from a perfectly conducting sphere are considered. The formulation of the problem in terms of the natural resonances of the sphere is the same as in Appendix B of Baum's note, and this is reviewed in the next section. Time domain curves of the current and charge at various points on the sphere are presented, as a function of the number of poles considered. The results of the conventional frequency domain-Fourier transform analysis are also given as a comparison.

It is hoped that this note, along with the others previously referenced, will provide a guide as to how the Singularity Expansion Method can be applied to EMP problems.

II. The Perfectly Conducting Sphere

In Appendix B of Ref. 1 the problem of electromagnetic scattering from a sphere is given in very general terms. In this section the equations from Ref. 1 are taken and stated in terms which can be conveniently used for numerical calculations. Throughout this note, equations referenced are those in Ref. 1, unless otherwise stated.

Equations B1 give the unit vectors for describing the plane wave incident on the sphere and are

$$\begin{aligned}
\vec{e}_1 &= \sin(\theta_1)\cos(\phi_1)\,\vec{e}_x + \sin(\theta_1)\sin(\phi_1)\,\vec{e}_y + \cos(\theta_1)\,\vec{e}_z \\
\vec{e}_2 &= -\cos(\theta_1)\cos(\phi_1)\,\vec{e}_x - \cos(\theta_1)\sin(\phi_1)\,\vec{e}_y + \sin(\theta_1)\,\vec{e}_z \\
\vec{e}_3 &= \sin(\phi_1)\,\vec{e}_x - \cos(\phi_1)\,\vec{e}_y
\end{aligned} \tag{1}$$

A convenient orientation for numerical calculation would be such that $\vec{e}_1 = \vec{e}_z$, $\vec{e}_2 = \vec{e}_x$, and $\vec{e}_3 = \vec{e}_y$. To accomplish this θ_1 must be 0 and ϕ_1 must be π. The convenience of such a coordinate system is that many of the terms involving the spherical harmonics will drop out or simplify. Fig. B1 in Ref. 1 represents the coordinate system in general, and Fig. 1 in this note shows the special orientation of the incident field. In this note, as in Ref. 1, the primed coordinates refer to the object coordinates.

Equation B99 is the frequency domain step function response for the surface current density and is given as

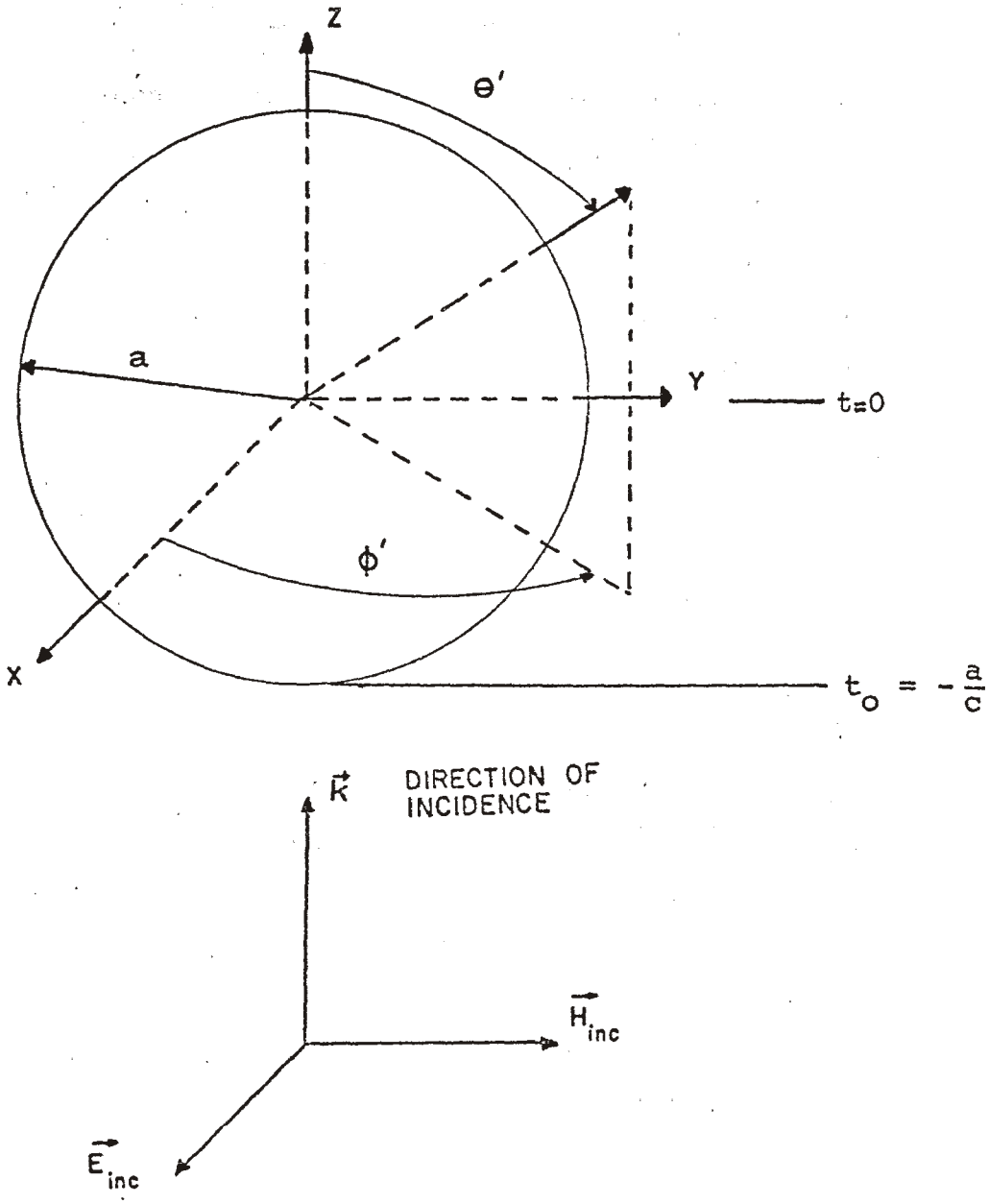

Figure 1. Plane Wave Incident on Perfectly Conducting Sphere.

$$\tilde{\vec{V}}_p^{(\vec{J}_s)}(\vec{r}', s) \equiv \tilde{\vec{V}}_{p_w}^{(\vec{J}_s)}(\vec{r}', s) + \tilde{\vec{V}}_{p_o}^{(\vec{J}_s)}(\vec{r}', s)$$

$$\tilde{\vec{V}}_{p_w}^{(\vec{J}_s)}(\vec{r}', s) = \frac{e^{-st_o}}{s} \tilde{\vec{U}}_p^{(\vec{J}_s)}(\vec{r}', 0) \tag{2}$$

$$\tilde{\vec{V}}_{p_o}^{(\vec{J}_s)}(\vec{r}', s) = e^{-st_o} \sum_{q=1}^{2} \sum_{n=1}^{\infty} \sum_{m=0}^{n} \sum_{\sigma=e,o} \sum_{\substack{n'=-\lambda\left(\frac{n+q-1}{2}\right) \\ n'\neq 0 \text{ for } n+q \text{ odd}}}^{\lambda\left(\frac{n+q-1}{2}\right)} \left[\frac{1}{s_{q,n,n'}} \right.$$

$$\left. c_{q,n,n',m,\sigma,p}(\theta_1, \phi_1) \vec{\nu}_{q,n,m,\sigma}^{(\vec{J}_s)}(\theta', \phi') \frac{1}{s - s_{q,n,n'}} \right]$$

Consider first the various factors defining $\tilde{\vec{V}}_{p_o}^{(\vec{J}_s)}(\vec{r}', s)$. The $s_{q,n,n'}$ are the natural frequencies and are discussed in Appendix B, pp. 93-100. Granzow[6] tabulates the $(s_{q,n,n'} \frac{a}{c})$ in his note. For this numerical work, Granzow's computer program which generates the $s_{q,n,n'}$ was modified to punch the numbers on data cards. Several checks were performed to insure accuracy. Figure 2 depicts the natural frequencies occurring in the upper left quadrant of the complex frequency plane.

The $c_{q,n,n',m,\sigma,p}(\theta_1, \phi_1)$ are the coupling coefficients. In this problem the $\vec{e}_p$ is the direction of the static electric field. The p subscript is chosen such that $\vec{E}_{inc}$ lies along the x-axis, so p must be 2. The coupling coefficient is then $c_{q,n,n',m,\sigma,2}(0, \pi)$. This may be broken down with Eq. B98, B58, and B56 as follows

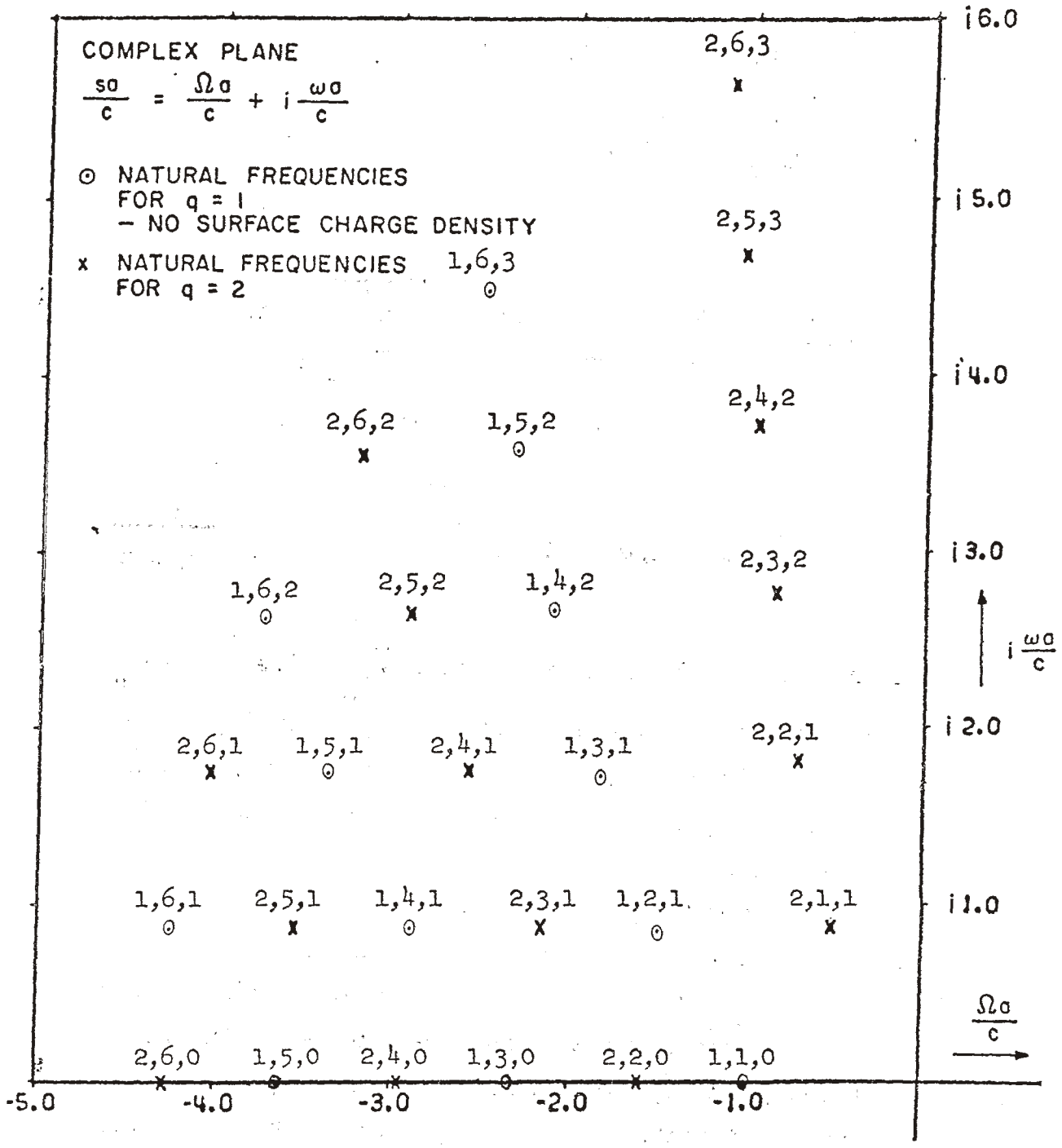

Figure 2. Natural Frequencies of the Perfectly Conducting Sphere for Use With Exterior Incident Wave. $1 \leq n \leq 6$

For q = 1

$$c_{1,\,n,\,n',\,m,\,\sigma,\,2}(0,\,\pi) = a'_{n,\,m,\,\sigma}\,D_{q,\,n,\,n'} \tag{3}$$

where

$$a'_{n,\,m,\,\substack{e\\o}} = (2-\delta_{o,\,m})(-1)^{n+1}\,\frac{(2n+1)(n-m)!}{n(n+1)(n+m)!}\,m\,\frac{P_n^m(\cos(0))}{\sin(0)}\begin{Bmatrix}-\sin(m\pi)\\ \cos(m\pi)\end{Bmatrix} \tag{4}$$

The even terms drop out due to the factor $\sin(m\pi) = 0$.

Now[7]

$$P_n^m(\cos(\alpha)) = (-1)^m \sin^m(\alpha)\,\frac{d^m P_n(\cos(\alpha))}{d(\cos(\alpha))^m} \tag{5}$$

so,

$$\frac{P_n^m(\cos(\alpha))}{\sin(\alpha)} = (-1)^m \sin^{m-1}(\alpha)\,\frac{d^m P_n(\cos(\alpha))}{d(\cos(\alpha))^m} \tag{6}$$

It can be said, since $\alpha = 0$, that the right hand side of this expression is 0 for all values of m except 1, where the $\sin(\alpha)$ term is indeterminate. Evaluating this for m = 1,

$$\lim_{\alpha \to 0} (\sin(\alpha))^0 = 1 \tag{7}$$

Therefore

$$\frac{P_n^1(\cos(\alpha))}{\sin(\alpha)} = -\left.\frac{d\,P_n(\cos(\alpha))}{d(\cos(\alpha))}\right|_{\alpha=0} \tag{8}$$

From Van Bladel[8]

$$\left.\frac{d\,P_n(\cos(\alpha))}{d(\cos(\alpha))}\right|_{\alpha=0} = \frac{n(n+1)}{2} \tag{9}$$

so,

$$\left.\frac{P_n^1(\cos(\alpha))}{\sin(\alpha)}\right|_{\alpha=0} = \frac{-n(n+1)}{2} \tag{10}$$

Since m = 1, the coupling coefficient now becomes

$$c_{1,\,n,\,n',\,1,\,o,\,2}(0,\,\pi) = (-1)^{n+1}\,\frac{(2n+1)}{n(n+1)}\,D_{1,\,n,\,n'} \tag{11}$$

For q = 2,

$$c_{2,\,n,\,n',\,m,\,\sigma,\,2}(0,\,\pi) = -b'_{n,\,m,\,\sigma}\,D_{2,\,n,\,n'} \tag{12}$$

where

$$-b'_{n,\,m,\,\begin{matrix}e\\o\end{matrix}} = (2-\delta_{o,\,m})(-1)^{n+1}\,\frac{(2n+1)}{n(n+1)}\,\frac{(n-m)!}{(n+m)!}\,\frac{d\,P_n^m(\cos(\theta_1))}{d(\theta_1)}\,\begin{Bmatrix}\cos(m\pi)\\ \sin(m\pi)\end{Bmatrix} \tag{13}$$

This time the odd terms drop out, since $\sin(m\pi) = 0$. Now,

$$\frac{dP_n^m(\cos(\alpha))}{d(\alpha)} = \frac{dP_n^m(\cos(\alpha))}{\frac{1}{-\sin(\alpha)}\,d(\cos(\alpha))} = -\sin(\alpha)\,\frac{dP_n^m(\cos(\alpha))}{d(\cos(\alpha))} \tag{14}$$

In Ref. 7, the recurrence relationship

$$(z^2-1)\,\frac{dP_n^m(z)}{dz} = nz\,P_n^m(z) - (n+m)\,P_{n-1}^m(z) \tag{15}$$

is given. Letting $z = \cos(\alpha)$,

$$-\sin^2(\alpha)\,\frac{dP_n^m(\cos(\alpha))}{d(\cos(\alpha))} = n\cos(\alpha)\,P_n^m(\cos(\alpha)) - (n+m)\,P_{n-1}^m(\cos(\alpha)) \tag{16}$$

so,

$$-\sin(\alpha)\frac{dP_n^m(\cos(\alpha))}{d(\cos(\alpha))} = n\cos(\alpha)\left[\frac{P_n^m(\cos(\alpha))}{\sin(\alpha)}\right] - (n+m)\left[\frac{P_{n-1}^m(\cos(\alpha))}{\sin(\alpha)}\right] \tag{17}$$

It can be seen that the terms in the brackets will be 0 except for m = 1 as above. This leaves

$$-\sin(\alpha)\frac{dP_n^1(\cos(\alpha))}{d(\cos(\alpha))} = n(\cos(\alpha))\left[\frac{P_n^1(\cos(\alpha))}{\sin(\alpha)}\right] - (n+1)\left[\frac{P_{n-1}^1(\cos(\alpha))}{\sin(\alpha)}\right] \tag{18}$$

Evaluating this at $\alpha = 0$ gives

$$-\sin(\alpha)\frac{dP_n^1(\cos(\alpha))}{d(\cos(\alpha))}\bigg|_{\alpha=0} = n\left[\frac{-n(n+1)}{2}\right] - (n+1)\left[\frac{-(n-1)(n)}{2}\right] = \frac{-n(n+1)}{2} \tag{19}$$

The coupling coefficient for q = 2 is therefore,

$$c_{2,n,n',1,e,2}(0,\pi) = (-1)^{n+1}\frac{(2n+1)}{n(n+1)}D_{2,n,n'} \tag{20}$$

Note that the factor in front of the $D_{q,n,n'}$ is the same for q = 1 and q = 2. The $D_{q,n,n'}$ are given in Eq. B82 and are the reciprocals of the first derivatives of the C coefficients, given in B 76, evaluated at the poles.

From B76,

$$C_{1,n}(\xi) = \xi \sum_{\beta=0}^{n} \frac{(n+\beta)!}{\beta!(n-\beta)!} (2\xi)^{-\beta} = \sum_{\beta=0}^{n} \frac{(n+\beta)!\, 2^{-\beta}}{\beta!(n-\beta)!} \xi^{-\beta+1} \tag{21}$$

$$\frac{dC_{1,n}(\xi)}{d\xi} = \sum_{\beta=0}^{n} \frac{(n+\beta)!\, 2^{-\beta}}{\beta!(n-\beta)!} \left[(1-\beta)\xi^{-\beta}\right] = 1 + \sum_{\beta=2}^{n} \frac{(n+\beta)!}{\beta!(n-\beta)!} (2\xi)^{-\beta}(1-\beta)$$

and

$$D_{1,n,n'} = \left. \frac{c/a}{1 + \sum_{\beta=2}^{n} \frac{(n+\beta)!}{\beta!(n-\beta)!} (2\xi)^{-\beta}(1-\beta)} \right|_{\xi = s_{1,n,n'}\frac{a}{c}} \tag{22}$$

Similarly,

$$C_{2,n}(\xi) = -\xi \sum_{\beta=0}^{n} \frac{(n+\beta)!\,(2\xi)^{-\beta}}{\beta!(n-\beta)!} - 2\xi \sum_{\beta=1}^{n} \beta \frac{(n+\beta)!}{\beta!(n-\beta)!} (2\xi)^{-\beta-1}$$

$$= -\xi - \sum_{\beta=1}^{n} \frac{(n+\beta)!}{\beta!(n-\beta)!} (2\xi)^{-\beta}(\xi+\beta) \tag{23}$$

$$\frac{dC_{2,n}(\xi)}{d\xi} = -1 - \sum_{\beta=1}^{n} \frac{(n+\beta)!}{\beta!(n-\beta)!} (2\xi)^{-\beta} + (\xi+\beta)(-2\beta(2\xi)^{-\beta-1})$$

$$= -1 - \sum_{\beta=1}^{n} \frac{(n+\beta)!}{\beta!(n-\beta)!} (2\xi)^{-\beta}\left(1 - \beta - \frac{\beta^2}{\xi}\right) \tag{24}$$

and

$$D_{2,n,n'} = \left. \frac{-c/a}{1 + \sum_{\beta=1}^{n} \frac{(n+\beta)!}{\beta!(n-\beta)!} (2\zeta)^{-\beta} (1 - \beta - \beta^2/\zeta)} \right|_{\zeta = s_{2,n,n'} \frac{a}{c}} \tag{24}$$

Table 1 at the end of this section presents the numerical values of the $(s_{q,n,n'} \frac{a}{c})$, $(D_{q,n,n'} \frac{a}{c})$, and $(c_{q,n,n',1,\sigma,2}(0,\pi)\frac{a}{c})$ for all poles up to and including n = 15. The n' given are for $n' \geq 0$, since the negative index simply gives the complex conjugate value, and there is only a single pole when the n' index is 0.

The next factor in the expansion is the natural mode vector, Eq. B88,

$$\vec{\nu}^{(\vec{J}_s)}_{q,n,m,\sigma}(\theta', \phi') = \left\{ \begin{array}{l} \vec{R}_{n,m,\sigma}(\theta', \phi') \quad \text{for } q = 1 \\ \vec{Q}_{n,m,\sigma}(\theta', \phi') \quad \text{for } q = 2 \end{array} \right\} \tag{25}$$

From the coupling coefficients, it was seen that m can only be 1. Also for q = 1, only the odd σ can be considered and for q = 2 the even σ, all other combinations giving 0. From this and B13

$$\vec{R}_{n,1,0}(\theta', \phi') = \vec{e}_{\theta'} \frac{P_n^1(\cos(\theta'))}{\sin(\theta')} \cos(\phi') - \vec{e}_{\phi'} \frac{dP_n^1(\cos(\theta'))}{d\theta'} \sin(\phi') \tag{26}$$

The theta component is therefore,

$$\left(R_{n,1,0}(\theta', \phi')\right)_{\theta'} = \cos(\phi') \frac{P_n^1(\cos(\theta'))}{\sin(\theta')} \tag{27}$$

and the phi component

$$\left(R_{n,1,0}(\theta',\phi')\right)_{\phi'} = -\sin(\phi')\frac{dP_n^1(\cos(\theta'))}{d\theta'}$$

$$= \sin(\phi')\left[\sin(\theta')\frac{dP_n^1(\cos(\theta'))}{d(\cos(\theta'))}\right] \tag{28}$$

Similarly, from B13

$$\vec{Q}_{n,1,e}(\theta',\phi') = \vec{e}_{\theta'}\frac{dP_n^1(\cos(\theta'))}{d\theta'}\cos(\phi') - \vec{e}_{\phi}\frac{P_n^1(\cos(\theta'))}{\sin(\theta')}\sin(\phi') \tag{29}$$

The theta component is

$$\left(Q_{n,1,e}(\theta',\phi')\right)_{\theta'} = \cos(\phi')\left(-\sin(\theta')\frac{dP_n^1(\cos(\theta'))}{d(\cos(\theta'))}\right) \tag{30}$$

and the phi component is

$$\left(Q_{n,1,e}(\theta',\phi')\right)_{\phi'} = \sin(\phi')\left[-\frac{P_n^1(\cos(\theta'))}{\sin(\theta')}\right] \tag{31}$$

In evaluating the Legendre functions the subroutine from Mathematics Note 3[9] is used except when $\theta' = 0$ and $\theta' = \pi$. It can be seen from Eq. (10) and Eq. (19) what the values are for $\theta' = 0$. From Harrington[10]

$$\left.\frac{P_n^1(\cos(\alpha))}{\sin(\alpha)}\right|_{\alpha=\pi} = \frac{(-1)^n}{2}n(n+1) \tag{32}$$

and

$$\left.\sin(\alpha)\frac{dP_n^1(\cos(\alpha))}{d(\cos(\alpha))}\right|_{\alpha=\pi} = \frac{(-1)^n}{2}n(n+1) \tag{33}$$

This completes the breakdown of the factors in the $\overrightarrow{\overrightarrow{V}}_{p_o}^{(\vec{J}_s)}(\vec{r}', s)$ of Eq. B99. The waveform part is

$$\overrightarrow{\overrightarrow{V}}_{p_w}^{(\vec{J}_s)}(\vec{r}', s) = \frac{e^{-st_o}}{s} \overrightarrow{\overrightarrow{U}}_{p}^{(\vec{J}_s)}(\vec{r}', 0) \tag{34}$$

The static response is, from B101, with m = 1, and σ odd

$$\begin{aligned} \overrightarrow{\overrightarrow{U}}_{2}^{(\vec{J}_s)}(\vec{r}', 0) &= A_{1,1,1,0,2} \vec{R}_{1,1,0}(\theta', \phi') \\ &= \frac{3}{2}\left[\vec{e}_{\theta'}\left(\frac{P_1^1(\cos(\theta'))}{\sin(\theta')}\cos(\phi')\right) + \vec{e}_{\phi'}\left(\sin(\theta')\frac{dP_1^1(\cos(\theta'))}{d(\cos(\theta'))}\sin(\phi')\right)\right] \end{aligned} \tag{35}$$

For the theta component,

$$\frac{P_1^1(\cos(\theta'))}{\sin(\theta')} = \frac{-\sin(\theta')}{\sin(\theta')} = -1 \tag{36}$$

So, the theta component of the static term is simply $-3/2 \cos(\phi')$. For the phi component

$$\begin{aligned} \frac{dP_1^1(\cos(\theta'))}{d(\cos(\theta'))} &= \frac{d(-\sin(\theta'))}{d(\cos(\theta))} \\ &= \frac{\cos(\theta')}{\sin(\theta')} \end{aligned} \tag{37}$$

The phi component of the static term is then $3/2 \sin(\phi') \cos(\theta')$.

Note that in all the factors having vectors, a term $\cos(\phi')$ may be factored out of the theta components and a $\sin(\phi')$ out of the phi component, so that all ϕ' dependence may be factored out from the currents.

The $\overleftrightarrow{V}_p^{(\vec{J}_s)}(\vec{r}', s)$ of B99 may now be broken into components and stated as follows, to summarize, the theta component is

$$\frac{\left(\overleftrightarrow{V}_2^{(\vec{J}_s)}(\vec{r}', s)\right)_{\theta'}}{\cos(\phi')} = e^{-st_o}\left[\frac{\frac{-3}{2}}{s} + \sum_q \sum_n \sum_{n'} \frac{1}{s_{q,n,n'}} C'_{q,n,n'} \left(\chi_{q,n}(\theta')\right)_{\theta'} \frac{1}{s - s_{q,n,n'}}\right] \tag{38}$$

where the χ function is one component of the mode vector with no ϕ' dependence. So, for $q = 1$

$$\left(\chi_{1,n}(\theta')\right)_{\theta'} = \frac{\left(\nu_{1,n,1,0}^{(\vec{J}_s)}(\theta', \phi')\right)_{\theta'}}{\cos(\phi')} = \frac{P_n^1(\cos(\theta'))}{\sin(\theta')} \tag{39}$$

and for $q = 2$

$$\left(\chi_{2,n}(\theta')\right)_{\theta'} = \frac{\left(\nu_{2,n,1,e}^{(\vec{J}_s)}(\theta', \phi')\right)_{\theta'}}{\cos(\phi')} = -\sin(\theta') \frac{d P_n^1(\cos(\theta'))}{d(\cos(\theta'))} \tag{40}$$

For the phi component,

$$\frac{\left(\overleftrightarrow{V}_2^{(\vec{J}_s)}(\vec{r}', s)\right)_{\phi'}}{\sin(\phi')} = e^{-st_o}\left[\frac{3}{2}\frac{\cos(\theta')}{s} + \sum_q \sum_n \sum_{n'} \frac{1}{s_{q,n,n'}} C'_{q,n,n'} \left(\chi_{q,n}(\theta')\right)_{\phi'} \frac{1}{s - s_{q,n,n'}}\right] \tag{41}$$

where for q = 1,

$$\left(\chi_{1,\,n}(\theta')\right)_{\phi'} = \frac{\left(\nu^{(\vec{J}_s)}_{1,\,n,\,1,\,0}(\theta',\phi')\right)_{\phi'}}{\sin(\phi')} = \sin(\theta')\,\frac{d\,P_n^1(\cos(\theta'))}{d(\cos(\theta'))} \tag{42}$$

and for q = 2,

$$\left(\chi_{2,\,n}(\theta')\right)_{\phi'} = \frac{\left(\nu^{(\vec{J}_s)}_{2,\,n,\,1,\,e}(\theta',\phi')\right)_{\phi'}}{\sin(\phi')} = -\frac{P_n^1(\cos(\theta'))}{\sin(\theta')} \tag{43}$$

also,

$$C'_{q,\,n,\,n'} = (-1)^{n+1}\,\frac{(2n+1)}{n(n+1)}\,D_{q,\,n,\,n'} \tag{44}$$

where the $D_{q,\,n,\,n'}$ are given in Eq. (22) and (24). From Eq. B75, $t_o = -a/c$.

This completes the analysis of the equations in B99 for the special coordinate system used for the numerical calculations. Now the time domain equations must be considered. These are found in Eqs. 2.64, which are,

$$\vec{V}^{(\vec{J}_s)}_{p_o}(\vec{r}',t) = \sum_{\alpha_o} s^{-1}_{\alpha_o} c_{\alpha_o}\,(\vec{e}_1)\,\vec{\nu}^{(\vec{J}_s)}_{\alpha_o}(\vec{r}')\,e^{\Omega_{\alpha_o}(t-t_o)}\,u(t-t_o)$$

$$+\sum_{\alpha_+} 2\mathrm{Re}\left[s^{-1}_{\alpha_+} c_{\alpha_+}\,(\vec{e}_1)\,\vec{\nu}^{(\vec{J}_s)}_{\alpha_+}(\vec{r}')\,e^{i\omega_{\alpha_+}(t-t_o)}\right] e^{\Omega_{\alpha_+}(t-t_o)}\,u(t-t_o) \tag{45}$$

$$\vec{V}^{(\vec{J}_s)}_{p_w}(\vec{r}',t) = \vec{\vec{U}}^{(\vec{J}_s)}_{s}(\vec{r}')\cdot\left[\vec{e}_1 \times \vec{e}_p\right] u(t-t_o)$$

From 2.1

$$s_\alpha \equiv \Omega_\alpha + i\omega_\alpha \tag{46}$$

The natural frequencies, coupling coefficients and mode vectors are the same as in B99, so combining the object and waveform parts and separating into theta and phi components, the time waveform will be

$$\frac{\left(V_2^{(\vec{J}_s)}(\vec{r}', t)\right)_{\theta'}}{\cos(\phi')} = \left[-\frac{3}{2} + \sum_q \sum_n \sum_{n'} \frac{1}{s_{q,n,n'}} C'_{q,n,n'} \left(\chi_{q,n}(\theta')\right)_{\theta'} e^{s_{q,n,n'}(t-t_o)}\right] u(t-t_o)$$

$$\frac{\left(V_2^{(\vec{J}_s)}(\vec{r}', t)\right)_{\phi'}}{\sin(\phi')} = \left[\frac{3}{2}\cos(\theta') + \sum_q \sum_n \sum_{n'} \frac{1}{s_{q,n,n'}} C'_{q,n,n'} \left(\chi_{q,n}(\theta')\right)_{\phi'} e^{s_{q,n,n'}(t-t_o)}\right] u(t-t_o) \tag{47}$$

where the $C'_{q,n,n'}$, $\left(\chi_{q,n}(\theta')\right)_{\theta'}$, and $\left(\chi_{q,n}(\theta')\right)_{\phi'}$, are the same as defined above.

The limits on the summations will depend on what is to be considered in any given case. The q index goes between 1 and 2. n will range between 1 and infinity, and the limits on n' are given in B79. In this note a given n is taken and the calculations will include all the poles up through and including those in that order and then adding individual poles (or pole pairs) in the n+1 order to observe their effect on the waveform. If a pole does not occur on the real axis ($i\omega \neq 0$) then it and its complex conjugate must both be included.

Now that current has been considered one may go on to the charge density. This is given in B100 as

$$\tilde{V}_p^{(\rho_s)}(\vec{r}', s) \equiv \tilde{V}_{p_w}^{(\rho_s)}(\vec{r}', s) + \tilde{V}_{p_o}^{(\rho_s)}(\vec{r}', s)$$

$$\tilde{V}_{p_w}^{(\rho_s)}(\vec{r}', s) = \frac{e^{-st_o}}{s} \tilde{U}_p^{(\rho_s)}(\vec{r}', 0)$$

$$\tilde{V}_{p_o}^{(\rho_s)}(\vec{r}', s) = e^{-st_o} \sum_{n=1}^{\infty} \sum_{m=0}^{n} \sum_{\sigma=e,o} \sum_{n'=-\lambda\left(\frac{n+1}{2}\right)}^{\lambda\left(\frac{n+1}{2}\right)} \left[\frac{c}{s^2_{2,n,n'} a_n} \right.$$

$$n' \neq 0 \text{ for } n \text{ odd}$$

$$\left. c_{2,n,n',m,\sigma,p}(\theta_1, \phi_1) \nu^{(\rho_s)}_{2,n,m,\sigma}(\theta', \phi') \frac{1}{s - s_{2,n,n'}} \right] \tag{48}$$

The coupling coefficient is the same as for current when q = 2, Eq. 20, which means only the m = 1 terms with σ even may be considered, all others being 0.

From B96

$$a_n = n(n+1)a \tag{49}$$

The natural mode term is, from B89,

$$\nu^{(\rho_s)}_{2,n,1,e}(\vec{r}') = Y_{n,1,e}(\theta', \phi')$$

$$= \cos(\phi') P_n^1(\cos(\theta')) \tag{50}$$

If $\theta' = 0$ or $\theta' = \pi$ the natural mode term is 0 since $P_n^1(\pm 1) = 0$, so θ' must be values other than 0 or π.

The static term is, from B104, with m = 1 and σ even

$$\tilde{U}_2^{(\rho_s)}(\vec{r}, 0) = 2A_{2, 1, 1, e, 2}\, Y_{1, 1, e}(\theta', \phi') \tag{51}$$

From B58 and B56

$$A_{2, 1, 1, e, 2} = b'_{1, 1, e} = -\frac{3}{2}$$

so

$$\begin{aligned}\tilde{U}_2^{(\rho_s)}(\vec{r}, 0) &= -3\cos(\phi')P_1^1(\cos(\theta')) \\ &= \cos(\phi')(3\sin(\theta'))\end{aligned} \tag{52}$$

Now rewrite B100 as

$$\frac{\tilde{V}_2^{(\rho_s)}(\vec{r}', s)}{\cos(\phi')} = e^{-st_o}\left(\frac{3\sin(\theta')}{s} + \sum_n \sum_{n'} \frac{n(n+1)\,c/a}{s^2_{2, n, n'}}\, C'_{2, n, n'} P_n^1(\cos(\theta'))\, \frac{1}{s - s_{2, n, n'}}\right) \tag{53}$$

where $C'_{2, n, n'}$ is given in Eq. 44.

The time domain expression will be

$$\frac{\tilde{V}_2^{(\rho_s)}(\vec{r}', t)}{\cos(\phi')} = \left(3\sin(\theta') + \sum_n \sum_{n'} \frac{n(n+1)\,c/a}{s^2_{2, n, n'}}\, C'_{2, n, n'} P_n^1(\cos(\theta'))\, e^{s_{2, n, n'}(t - t_o)}\right) u(t - t_o) \tag{54}$$

where again the summation limits are as before.

The surface current and charge density step response functions are now in a form which can be programmed for calculations on a digital computer. In this note the calculations for the frequency domain step response functions are multiplied by s (ika in the normalized frequency spectrum). The difference between this and the delta response function is discussed in Section IV.

n	n'	$s_{1,n,n'}a/c$		$D_{1,n,n'}a/c$		$c_{1,n,n',1,0,2}^{(0,\pi)}a/c$	
		real	imaginary	real	imaginary	real	imaginary
1	0	-1.0000	0.0000	1.0000	0.0000	1.5000	0.0000
2	1	-1.5000	.8660	.5000	.8660	-.4167	-.7217
3	0	-2.3222	0.0000	1.6285	0.0000	.9499	0.0000
3	1	-1.8389	1.7544	-.3142	.9616	-.1833	.5609
4	1	-2.8962	.8672	1.4116	1.7555	-.6352	-.7900
4	2	-2.1038	2.6574	-.9116	.4919	.4102	-.2213
5	0	-3.6467	0.0000	3.9045	0.0000	1.4317	0.0000
5	1	-3.3520	1.7427	-.4110	2.8844	-.1507	1.0576
5	2	-2.3247	3.5710	-1.0412	-.2373	-.3818	-.0870
6	1	-4.2484	.8675	4.0506	4.4717	-1.2537	-1.3841
6	2	-3.7357	2.6263	-2.8791	2.2090	.8911	-.6837
6	3	-2.5159	4.4927	-.6715	-.8779	.2078	.2717
7	0	-4.9718	0.0000	10.7796	0.0000	2.8874	0.0000
7	1	-4.7583	1.7393	-.5262	8.6995	-.1410	2.3302
7	2	-4.0701	3.5172	-4.3908	-.4020	-1.1761	-.1077
7	3	-2.6857	5.4207	.0272	-1.1460	.0073	-.3070
8	1	-5.5879	.8676	12.2272	12.6837	-2.8870	-2.9948
8	2	-5.2048	2.6162	-8.8795	8.1230	2.0965	-1.9179
8	3	-4.3683	4.4144	-3.6036	-3.8343	.8509	.9053
8	4	-2.8390	6.3539	.7559	-.9194	-.1785	.2171
9	0	-6.2970	0.0000	32.0333	0.0000	6.7626	0.0000
9	1	-6.1294	1.7378	-.3618	27.1014	-.0764	5.7214
9	2	-5.6044	3.4982	-16.0822	-.1358	-3.3951	-.0287
9	3	-4.6384	5.3173	-.2772	-6.1874	-.0585	-1.3062
9	4	-2.9793	7.2915	1.2045	-.2790	.2543	-.0589
10	1	-6.9220	.8677	38.3290	38.2615	-7.3173	-7.3045
10	2	-6.6153	2.6116	-27.9335	28.4831	5.3328	-5.4377
10	3	-5.9675	4.3849	-15.4475	-14.1688	2.9491	2.7050
10	4	-4.8862	6.2250	4.3792	-5.7277	-.8360	1.0935
10	5	-3.1089	8.2327	1.1728	.5239	-.2239	-.1000

Table 1a. Natural Frequencies and Pole Expansion Terms for the Perfectly Conducting Sphere.
$q = 1$
$1 \leq n \leq 10$

n	n'	$s_{1,n,n'}a/c$		$D_{1,n,n'}a/c$		$c_{1,n,n',1,0,2}(0,\pi)a/c$	
		real	imaginary	real	imaginary	real	imaginary
11	0	-7.6223	0.0000	99.6026	0.0000	17.3550	0.0000
11	1	-7.4842	1.7371	1.5114	86.7723	.2633	15.1194
11	2	-7.0579	3.4890	-56.6944	2.6875	-9.8786	.4680
11	3	-6.3013	5.2762	-2.8656	-26.6266	-.4993	-4.6395
11	4	-5.1156	7.1370	8.0972	-1.8978	1.4109	-.3307
11	5	-3.2297	9.1771	.6501	1.1652	.1133	.2030
12	1	-8.2534	.8677	123.4916	120.0974	-19.7903	-19.2464
12	2	-7.9973	2.6091	-89.8188	98.6691	14.3940	-15.8124
12	3	-7.4656	4.3702	-60.6824	-49.9366	9.7247	8.0027
12	4	-6.6110	6.1715	19.1131	-27.7060	-3.0630	4.4401
12	5	-5.3297	8.0529	8.5734	4.1366	-1.3739	-.6629
12	6	-3.3430	10.1243	-.1768	1.3742	.0283	-.2202
13	0	-8.9477	0.0000	319.3543	0.0000	47.3767	0.0000
13	1	-8.8303	1.7367	11.1044	283.8186	1.6474	42.1050
13	2	-8.4706	3.4839	-197.6906	17.3112	-29.3277	2.5681
13	3	-7.8444	5.2549	-16.5672	-105.1183	-2.4578	-15.5945
13	4	-6.9004	7.0706	40.2773	-10.9052	5.9752	-1.6178
13	5	-5.5307	8.9722	4.6904	9.7539	.6958	1.4470
13	6	-3.4199	11.0739	-.9915	1.0419	-.1471	.1546
14	1	-9.5832	.8677	406.1225	387.5621	-56.0836	-53.5205
14	2	-9.3631	2.6076	-294.2717	341.4053	40.6375	-47.1464
14	3	-8.9110	4.3616	-228.9372	-173.4236	31.6151	23.9490
14	4	-8.1988	6.1430	75.2563	-119.7447	-10.3925	16.5362
14	5	-7.1724	7.9732	46.4561	21.3480	-6.4154	-2.9481
14	6	-5.7204	9.8947	-2.6581	11.9418	.3671	-1.6491
14	7	-3.5511	12.0257	-1.4679	.2688	.2027	-.0371
15	0	-10.2731	0.0000	1046.9179	0.0000	135.2269	0.0000
15	1	-10.1709	1.7364	52.1798	943.9529	6.7399	121.9273
15	2	-9.8596	3.4807	-688.2131	81.1837	-88.8942	10.4862
15	3	-9.3236	5.2423	-78.6977	-398.5534	-10.1651	-51.4798
15	4	-8.5325	7.0344	176.7443	-54.6047	22.8295	-7.0531
15	5	-7.4294	8.8790	27.0396	55.8020	3.4926	7.2078
15	6	-5.9002	10.8200	-10.6149	8.7526	-1.3711	1.1305
15	7	-3.6474	12.9795	-1.3970	-.6661	-.1804	-.0860

Table 1b. Natural Frequencies and Pole Expansion Terms for the Perfectly Conducting Sphere.
$q = 1$
$11 \leq n \leq 15$

n	n'	$s_{2,n,n'}a/c$		$D_{2,n,n'}a/c$		$c_{2,n,n',1,e,2}(0,\pi)a/c$	
		real	imaginary	real	imaginary	real	imaginary
1	1	-.5000	.8660	-.5000	-.2887	-.7500	-.4330
2	0	-1.5961	0.0000	-.6265	0.0000	.5221	0.0000
2	1	-.7020	1.8073	-.1867	-.4808	.1556	.4006
3	1	-2.1571	.8706	-.6330	-.5127	-.3692	-.2991
3	2	-.8429	2.7579	.1330	-.4715	.0776	-.2750
4	0	-2.9487	0.0000	-1.3236	0.0000	.5956	0.0000
4	1	-2.5714	1.7523	-.2127	-1.0072	.0957	.4532
4	2	-.9542	3.7148	.3746	-.2945	-.1686	.1325
5	1	-3.5443	.8689	-1.5392	-1.2729	-.5644	-.4667
5	2	-2.9081	2.6443	.5706	-1.1300	.2092	-.4143
5	3	-1.0477	4.6764	.4685	-.0216	.1718	-.0079
6	0	-4.2846	0.0000	-3.4713	0.0000	1.0745	0.0000
6	1	-4.0336	1.7430	-.5387	-2.8050	.1667	.8682
6	2	-3.1952	3.5449	1.3823	-.6408	-.4278	.1983
6	3	-1.1289	5.6416	.3921	.2501	-.1214	-.0774
7	1	-4.8972	.8684	-4.3041	-3.5865	-1.1529	-.9607
7	2	-4.4540	2.6233	1.8705	-3.4511	.5010	-.9244
7	3	-3.4476	4.4526	1.7559	.4089	.4703	.1095
7	4	-1.2012	6.6097	.1778	.4277	.0476	.1146
8	0	-5.6156	0.0000	-10.0314	0.0000	2.3685	0.0000
8	1	-5.4263	1.7398	-1.5530	-8.4287	.3667	1.9901
8	2	-4.8254	3.5095	4.8351	-1.9997	-1.1416	.4722
8	3	-3.6739	5.3662	1.3309	1.6302	-.3142	-.3849
8	4	-1.2666	7.5801	-.0973	.4525	.0230	-.1068
9	1	-6.2383	.8682	-12.9072	-10.7982	-2.7249	-2.2796
9	2	-5.8954	2.6153	6.1346	-10.9895	1.2951	-2.3200
9	3	-5.1598	4.4011	6.5316	1.9157	1.3789	.4044
9	4	-3.8798	6.2850	.0781	2.4279	.0165	.5126
9	5	-1.3266	8.5525	-.3371	.3180	-.0712	.0671

Table 1c. Natural Frequencies and Pole Expansion Terms for the Perfectly Conducting Sphere.
$q = 2$
$1 \leq n \leq 9$

n	n'	$s_{2,n,n'}a/c$		$D_{2,n,n'}a/c$		$c_{2,n,n',1,e,2}(0,\pi)a/c$	
		real	imaginary	real	imaginary	real	imaginary
10	0	-6.9444	0.0000	-30.6474	0.0000	5.8509	0.0000
10	1	-6.7922	1.7383	-4.7608	-26.4439	.9089	5.0484
10	2	-6.3191	3.4950	16.6591	-6.5288	-3.1804	1.2464
10	3	-5.4650	5.2977	4.9897	7.1036	-.9526	-1.3562
10	4	-4.0694	7.2081	-1.6052	2.2673	.3064	-.4328
10	5	-1.3821	9.5265	-.4592	.0722	.0877	-.0138
11	1	-7.5739	.8680	-40.3984	-33.8803	-7.0391	-5.9034
11	2	-7.2935	2.6113	20.3558	-35.8819	3.5469	-6.2522
11	3	-6.7067	4.3789	23.5834	7.5869	4.1092	1.3220
11	4	-5.7465	6.1987	-.6180	10.8721	-.1077	1.8944
11	5	-4.2453	8.1351	-3.0011	.9624	-.5229	.1677
11	6	-1.4339	10.5019	-.4218	-.1999	-.0735	-.0348
12	0	-8.2722	0.0000	-97.0834	0.0000	15.5582	0.0000
12	1	-8.1448	1.7375	-15.1467	-85.3830	2.4274	13.6832
12	2	-7.7532	3.4875	57.3518	-21.7857	-9.1910	3.4913
12	3	-7.0650	5.2668	18.3369	28.0990	-2.9386	-4.5030
12	4	-5.7084	7.1038	-8.6339	10.1075	1.4269	-1.6105
12	5	-4.4099	9.0655	-3.3587	-1.1532	.5382	.1848
12	6	-1.4825	11.4786	-.2378	-.4044	.0381	.0648
13	1	-8.9065	.8680	-130.1711	-109.3505	-19.3111	-16.2223
13	2	-8.6691	2.6090	68.3584	-119.2875	10.1411	-17.6965
13	3	-8.1787	4.3670	84.1582	28.4562	12.4850	4.2215
13	4	-7.3989	6.1583	-4.4472	44.3780	-.6597	6.5835
13	5	-6.2537	8.0125	-16.1760	3.0554	-2.3997	.4533
13	6	-4.5647	9.9990	-2.2524	-3.2782	-.3342	-.4863
13	7	-1.5284	12.4563	.0301	-.4709	.0045	-.0699

Table 1d. Natural Frequencies and Pole Expansion Terms for the Perfectly Conducting Sphere.
$q = 2$
$10 \leq n \leq 15$

n	n'	$s_{2,n,n'}a/c$		$D_{2,n,n'}a/c$		$c_{2,n,n',1,e,2}(0,\pi)a/c$	
		real	imaginary	real	imaginary	real	imaginary
14	0	-9.5994	0.0000	-315.4652	0.0000	43.5642	0.0000
14	1	-9.4898	1.7370	-49.4237	-281.4597	6.8252	38.8682
14	2	-9.1551	3.4831	198.1264	-73.7556	-27.3603	10.1853
14	3	-8.5758	5.2496	66.6335	106.6635	-9.2018	-14.7297
14	4	-7.7120	7.0533	-40.8105	41.6856	5.6357	-5.7566
14	5	-6.4847	8.9245	-17.7311	-9.0531	2.4486	1.2502
14	6	-4.7110	10.9351	.1475	-4.4290	-.0204	.6116
14	7	-1.5719	13.4351	.2905	-.3757	-.0401	.0519
15	1	-10.2373	.8679	-428.3704	-360.2875	-55.3312	-46.5371
15	2	-10.0312	2.6076	232.0063	-402.0841	29.9675	-51.9359
15	3	-9.6092	4.3598	299.0664	104.2944	38.6294	13.4714
15	4	-8.9486	6.1354	-21.8088	173.2352	-2.8170	22.3762
15	5	-8.0072	7.9516	-74.6609	9.3119	-9.6437	1.2028
15	6	-6.7033	9.8396	-10.2234	-21.5534	-1.3205	-2.7840
15	7	-4.8500	11.8737	3.0368	-3.8637	.3923	-.4991
15	8	-1.6133	14.4147	.4539	-.1503	.0586	-.0194

Table 1d. (Continued)

III. Classical Frequency Domain Approach

In this section, the conventional frequency domain-inverse Fourier transform solution is discussed. For the induced current on the sphere, Harrington develops the equations

$$J_\theta = \frac{i E_{inc}(ka)}{Z_o} \frac{\cos\phi}{ka} \sum_{n=1}^{\infty} a_n \left[\frac{\sin\theta \dfrac{dP_n^1(\cos\theta)}{d(\cos\theta)}}{\dfrac{d\hat{H}_n^{(2)}(ka)}{d(ka)}} + \frac{j P_n^1(\cos\theta)}{\sin\theta \hat{H}_n^{(2)}(ka)} \right] \tag{55}$$

and

$$J_\phi = \frac{i E_{inc}(ka)}{Z_o} \frac{\sin\phi}{ka} \sum_{n=1} a_n \left[\frac{P_n^1(\cos\theta)}{\sin\theta \dfrac{d\hat{H}_n^{(2)}(ka)}{d(ka)}} - \frac{\sin\theta \dfrac{dP_n^1(\cos\theta)}{d(\cos\theta)}}{j\hat{H}_n^{(2)}(ka)} \right] \tag{56}$$

Note that $\hat{H}_n^{(2)}(ka) = ka\, h_n^{(2)}(ka)$ where $h_n^{(2)}(ka)$ is the Hankel function and Z_o is the free space wave impedance. The spherical Hankel functions were evaluated with the subroutine in Mathematics Note 4.[11]

In Eq. (55) and (56),

$$a_n = i^n (2n + 1)/(n(n + 1)) \tag{57}$$

and P_n^1 is an associated Legendre function which may be evaluated using the subroutine from Ref. 9. Equations (10), (19), (32), and (33) were used to evaluate the values for $\theta = 0$ and $\theta = \pi$.

The infinite sums of Eqs. (55) and (56) were calculated with the convergence criteria of

$$\left| B_n / \sum_{i=1}^{n} B_i \right| \leq 1 \times 10^{-8} \tag{58}$$

where B_i is the n^{th} term of the series.

For the purpose of this note, $\vec{E}_{inc}(ka)$ was the transformed step function in time. In the frequency domain, $E_{inc}(ka) \sim E_o/ika$. With this value of $\vec{E}_{inc}(ka)$, Eqs. (55) and (56) were transformed into the time domain. All transformations were done using the fast Fourier transformation method.[12]

From the continuity equation,

$$\nabla \cdot \vec{J} + s\rho = 0 \tag{59}$$

The charge density is found to be

$$\rho = \epsilon_o \vec{E}_{inc}(ka) \cos(\phi) \frac{i}{(ka)^2} \sum_{n=1}^{\infty} \frac{(-i)^{n-2}(2n+1) P_n^1(\cos\theta)}{(\hat{H}^{(2)}(ka))'} \tag{60}$$

The results of these equations are compared to the natural mode method in Section IV.

IV. Numerical Results

The step function current density and charge density responses are given in Eqs. 38, 41, 47, 53, and 54 for both frequency and time domains. These equations are in terms of the $\tilde{\vec{V}}_p^{(\vec{J}_s)}(\vec{r}', t \text{ or } s)$ and $\tilde{V}_p^{(\rho_s)}(\vec{r}', t \text{ or } s)$. These may be written in terms of the current and charge densities. From 2.36 in Ref. 1,

$$\tilde{\vec{V}}_p^{(\vec{J}_s)}(\vec{r}', s) = \tilde{f}_p(s)\,\tilde{\vec{U}}_p^{(\vec{J}_s)}(\vec{r}', s) \tag{61}$$

and from 2.19, the current may be expressed as

$$\tilde{\vec{J}}_{s_p}(\vec{r}', s) = \frac{E_o}{Z_o}\tilde{f}_p(s)\,\tilde{\vec{U}}_p^{(\vec{J}_s)}(\vec{r}', s) = \frac{E_o}{Z_o}\tilde{\vec{V}}^{(\vec{J}_s)}(\vec{r}', s) \tag{62}$$

so for the theta and phi components of current

$$\begin{aligned} J_{s_{\theta'}}(s) &= \frac{E_o}{Z_o}\left(\tilde{V}_p^{(\vec{J}_s)}(\vec{r}', s)\right)_{\theta'} \\ J_{s_{\phi'}}(s) &= \frac{E_o}{Z_o}\left(\tilde{V}_p^{(\vec{J}_s)}(\vec{r}', s)\right)_{\phi'} \end{aligned} \tag{63}$$

Similarly, for charge,

$$\rho_s(s) = \epsilon_o E_o \tilde{V}_p^{(\rho_s)}(\vec{r}', s) \tag{64}$$

In this note the normalized frequency response is evaluated for s on the $i\omega$ axis, so that

$$s\frac{a}{c} = i\omega\frac{a}{c} = ika \tag{65}$$

The time domain results are also normalized by a/c, so that they are presented in terms of ct/a. The expressions evaluated are then, for frequency domain step function response times ika. These give a close approximation to the delta function response and are,

$$\frac{ika\, J_{s_{\theta'}}(ka)\, Z_o}{E_o \cos(\phi')} = \frac{ika}{\cos(\phi')}\left(\tilde{V}_p^{(\vec{J}_s)}(\vec{r}', ika)\right)_{\theta'}$$

$$\frac{ika\, J_{s_{\phi'}}(ka)\, Z_o}{E_o \sin(\phi')} = \frac{ika}{\sin(\phi')}\left(\tilde{V}_p^{(\vec{J}_s)}(\vec{r}', ika)\right)_{\phi'} \tag{66}$$

$$\frac{ika\, \rho_s(ka)}{\epsilon_o E_o \cos(\phi')} = \frac{ika}{\cos(\phi')}\,\tilde{V}_p^{(\rho_s)}(ika)$$

and for the time domain step function response

$$\frac{J_{s_{\theta'}}(ct/a)\, Z_o}{E_o \cos(\phi')} = \frac{\left(\tilde{V}_p^{(\vec{J}_s)}(\vec{r}', ct/a)\right)_{\theta'}}{\cos(\phi')}$$

$$\frac{J_{s_{\phi'}}(ct/a)\, Z_o}{E_o \cos(\phi')} = \frac{\left(\tilde{V}_p^{(\vec{J}_s)}(\vec{r}', ct/a)\right)_{\phi'}}{\sin(\phi')} \tag{67}$$

$$\frac{\rho_s(ct/a)}{\epsilon_o E_o \cos(\phi')} = \frac{\tilde{V}_p^{(\rho_s)}(ct/a)}{\cos(\phi')}$$

In evaluating the classical frequency domain approach the equations were normalized in this same fashion, so that direct comparisons could be made.

Figures 3 through 7 show the waveforms for the time domain equations (Eq. 63). Poles considered are all poles through a specific order, labeled N on the graphs. So, if N = 3, all poles up to and including n = 3 are included. The line labeled N = 0 is the static term. Orders up through 15 were studied; the graphs illustrate waveforms for orders n = 1, 2, 3, and 4. This is sufficient to show how the addition of poles contributes to the convergence of the current to the actual infinite limit.

The initial effect of the incident wave at the observation points considered ($\theta' = 0,\ \pi/4,\ \pi/2,\ 3\pi/4$, and π) is shown by the vertical dotted line. These time values may be determined by geometric optics. Note from Fig. 1 that time zero is at the center of the sphere. The "turn on" time for $\theta' = \pi$ will then be -a/c, and for $\theta' = 0$, $ct/a = 1 + \pi/2$. All graphs in the time domain begin with $ct/a = -1$.

On the "shadowed" side of the sphere ($0 \leq \theta' < \pi/2$) the N = 15 curve shows some very small oscillations along the zero axis until "turn on" time and then it follows the $N = \infty$ curve exactly. The classical frequency domain approach produces exactly the same numbers as for the N = 15 waveform. The curves labeled ∞ are those computed from the classical technique. For the illuminated side ($\pi/2 < \theta' \leq \pi$) the classical frequency approach produces a smooth curve from the "turn on" time; the singularity expansion method at N = 15 is still producing some oscillations at early time before converging to the infinite pole limit.

Figure 8 is the delta function response graphs for frequency domain at $\theta' = 3\pi/4$. These are the magnitudes of the complex functions in Eq. 66.

As more orders are included, the singularity expansion frequency spectrum more closely approaches the infinite pole limit. With fewer

poles, the frequency spectrum goes to zero sooner than in the case where more poles are added. As in the time domain graphs, the curves labeled "∞" are produced from the classical frequency domain approach. For N = 15 there is a "hump" which occurs at ct/a $\sim$ 15 and then the spectrum goes to 0. It is noted that for orders between N = 4 and N = 15, the waveform closely follows the ∞ curve until a certain point in frequency and then a "hump" occurs before it goes to zero. This is true for both "shadowed" and "illuminated" parts of the sphere. Fig. 8 includes curves for N = 15.

Figures 9 and 10 show, in the time domain, the effects of individual poles (or pole pairs if the poles are complex) on the waveform. For Fig. 9, poles of order 1 are added to the static term, and in Fig. 10, poles of order 2 are added to the waveform produced by all poles through order n = 1.

Note in Fig. 10 for the theta component of the current that $s_{2,2,0}$ and $s_{2,2,1}$ do not contribute anything to the N = 1 waveform. And similarly in the phi component $s_{1,2,1}$ does not contribute to the N = 1 curve. This effect can be seen from the mode vector $\vec{\nu}_{\alpha}^{(\vec{J}_s)}(\vec{r}')$. For q = 2 in the theta component, and from Eq. 40

$$\frac{\left(\nu_{2,n,1,e}^{(\vec{J}_s)}(\theta',\phi')\right)_{\theta'}}{\cos(\phi')} = -\sin(\theta') \left.\frac{d P_n^1(\cos(\theta'))}{d(\cos(\theta'))}\right|_{\substack{\theta'=3\pi/4 \\ n=2}} = 0 \qquad (68)$$

The same thing is true for q = 1 for the phi component. This implies that due to nulls in the natural modes of the sphere, not all of the natural frequencies contribute to the convergence of the waveforms at certain points on the body.

As was noted earlier in the note the frequency domain calculations for Fig. 8 are not strictly speaking the delta function response, but rather the step function response multiplied by ika. The actual delta function response of Eq. B97 was also calculated for comparison. It was interesting to note that when all the poles for a given order are included, along with all poles for lower orders; the two calculations differed only by a relative difference of about 10^{-3} for values of n up to 15 and ka to 15. When only a few poles are included in an order, the two calculations did vary considerably.

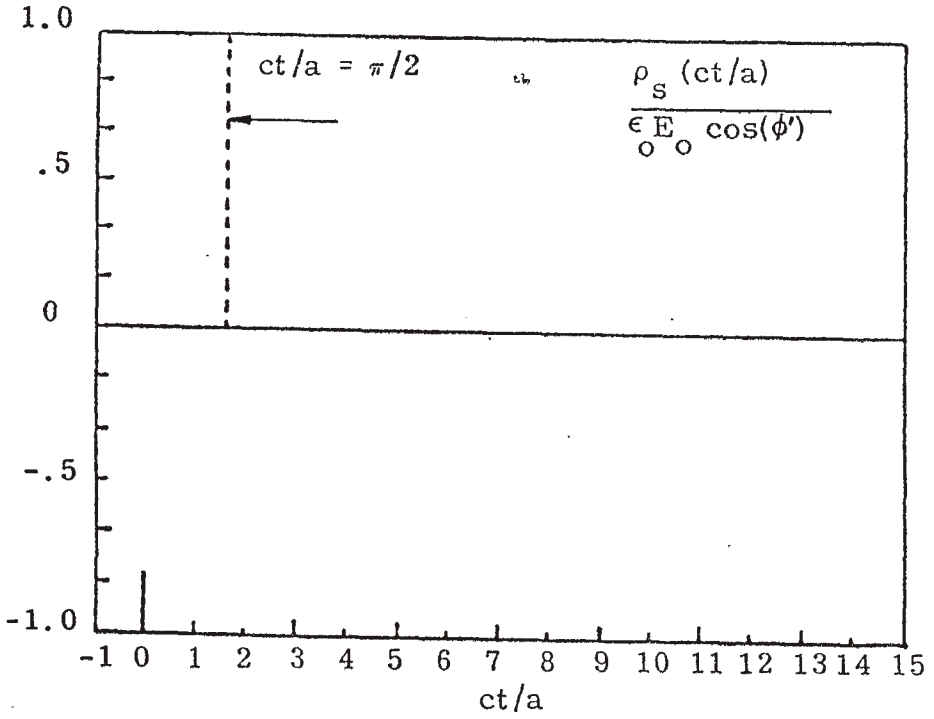

Surface Charge Density

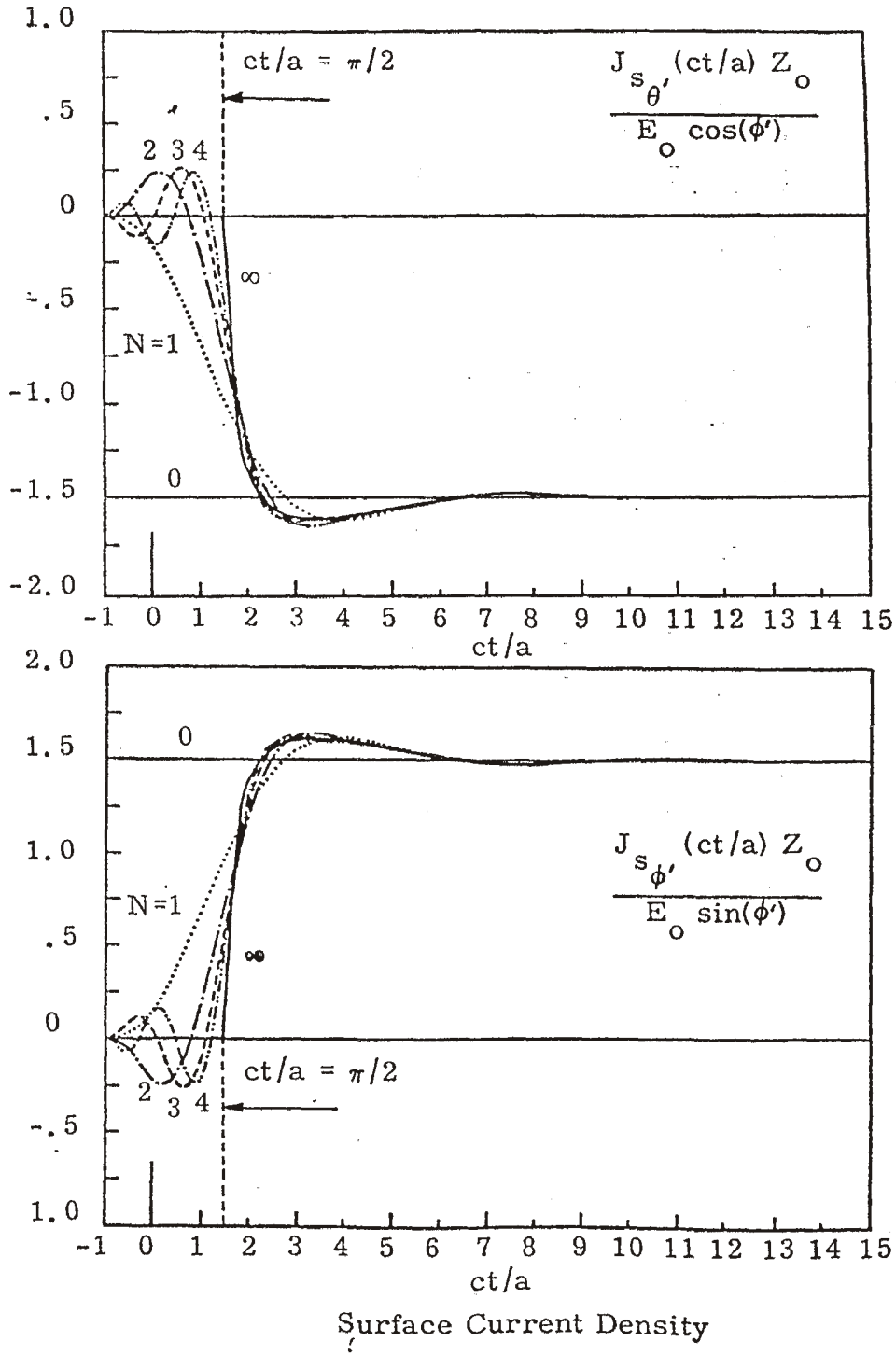

Surface Current Density

Figure 3. Step Function Response for Surface Current and Charge Densities. $\theta' = 0$.

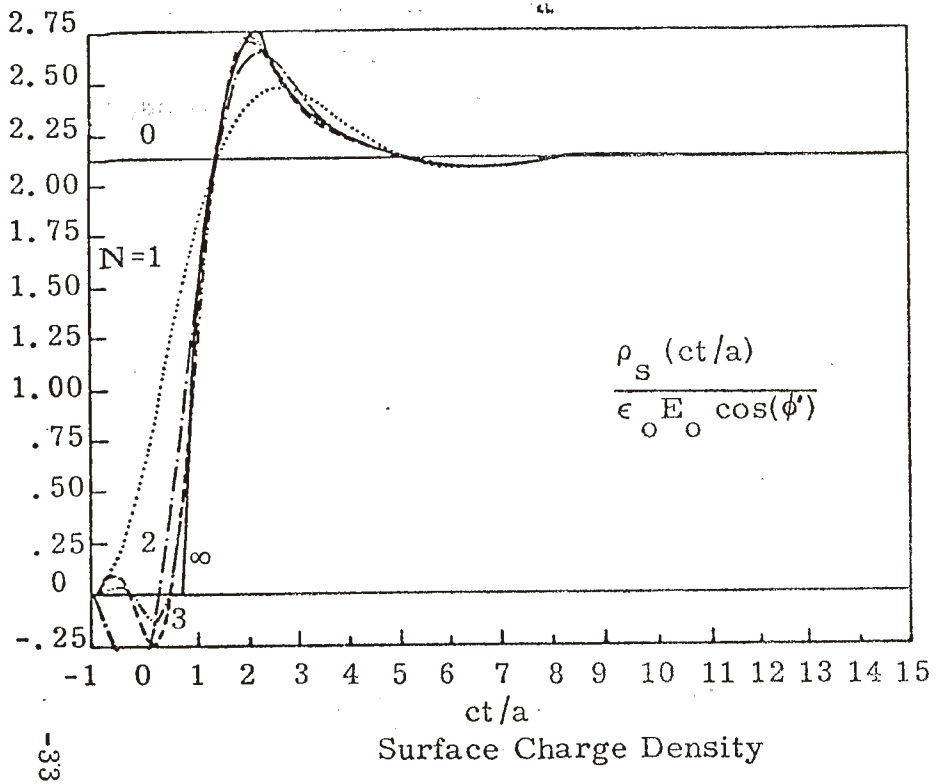

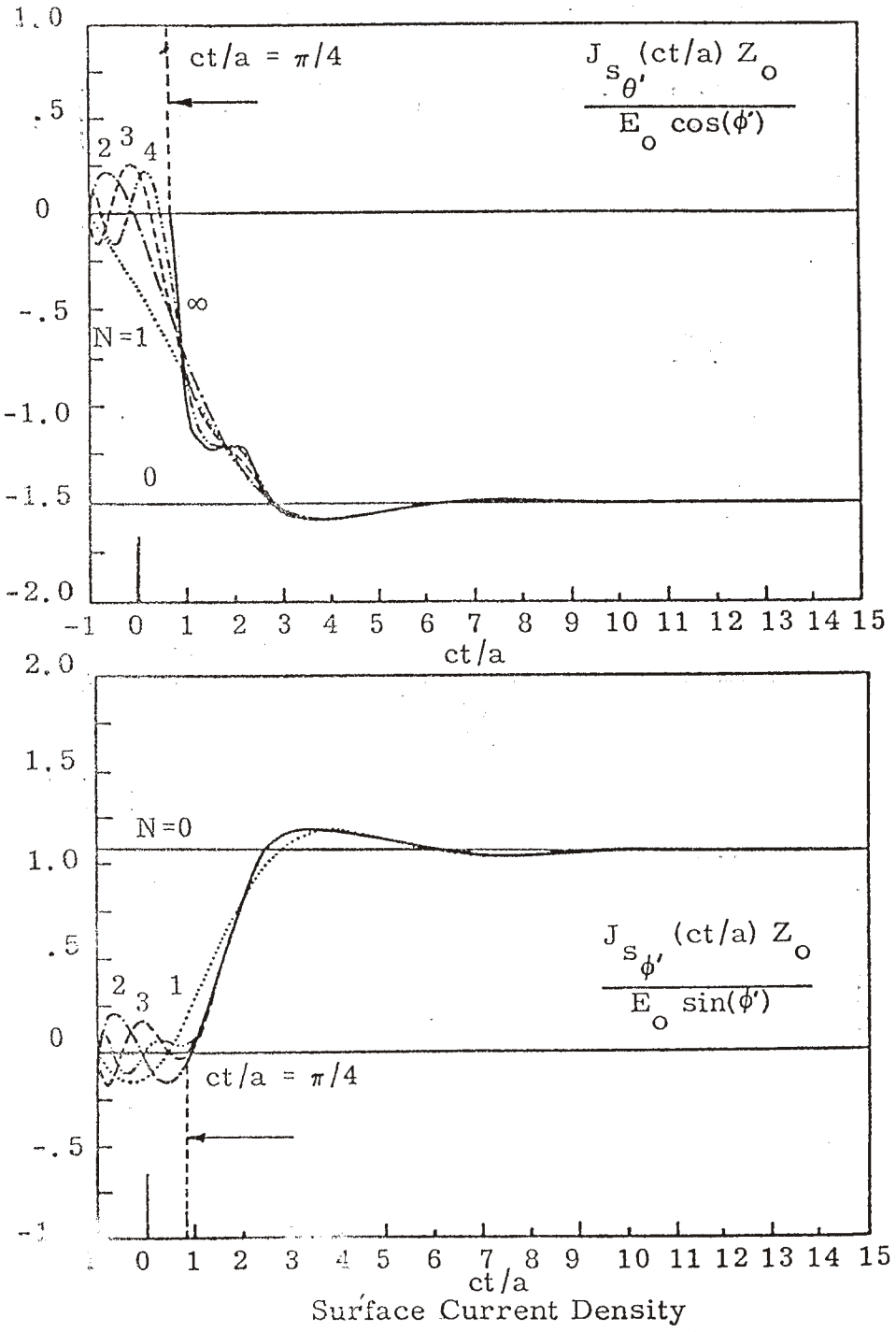

Figure 4. Step Function Response for Surface Current and Charge Densities. $\theta' = \pi/4$.

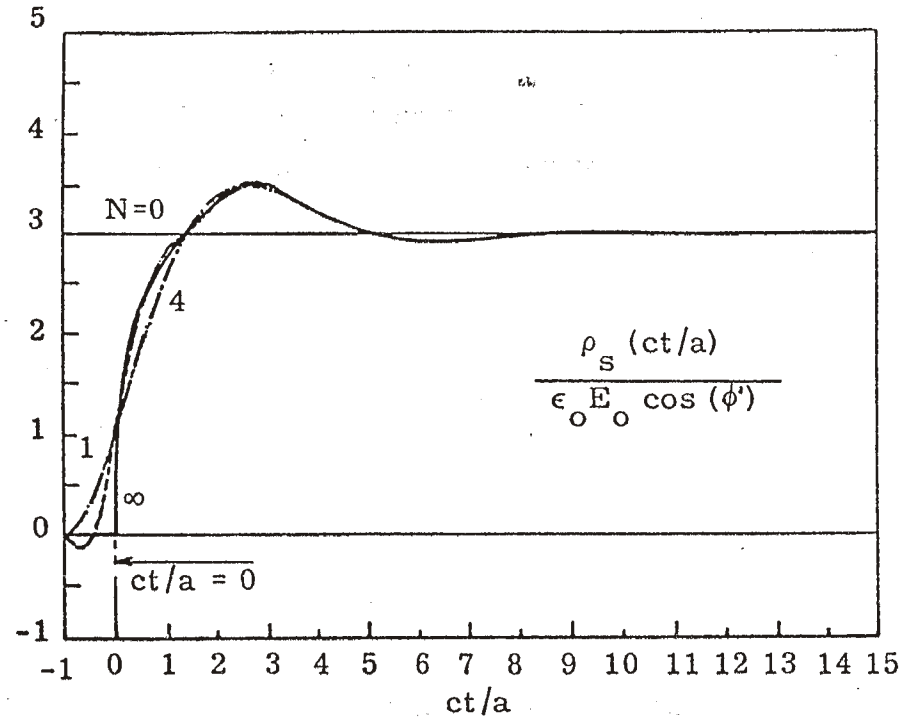

Surface Charge Density

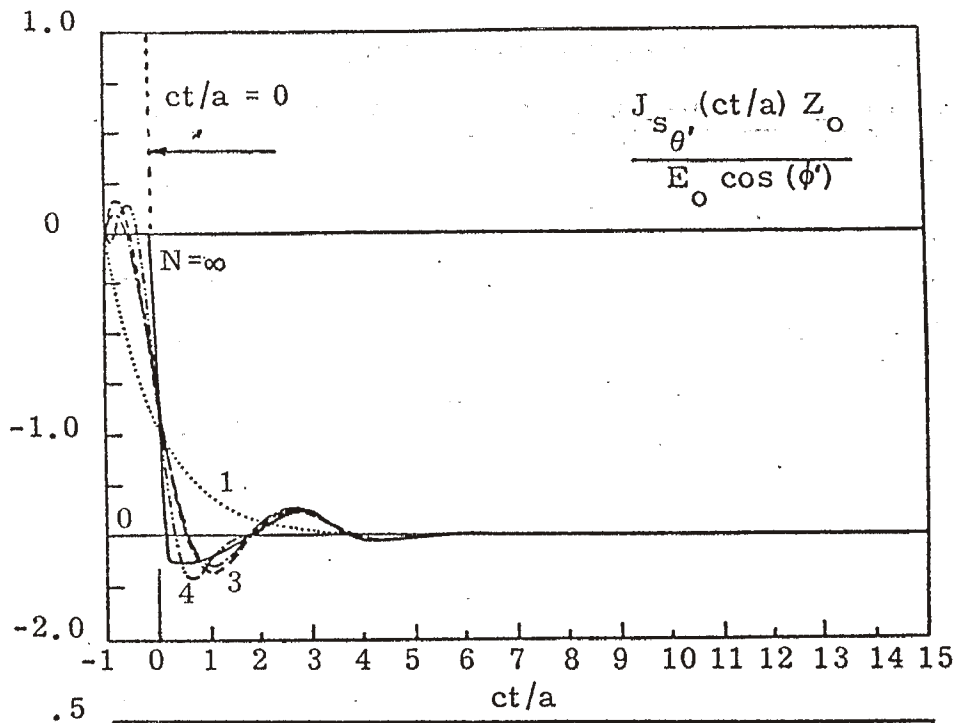

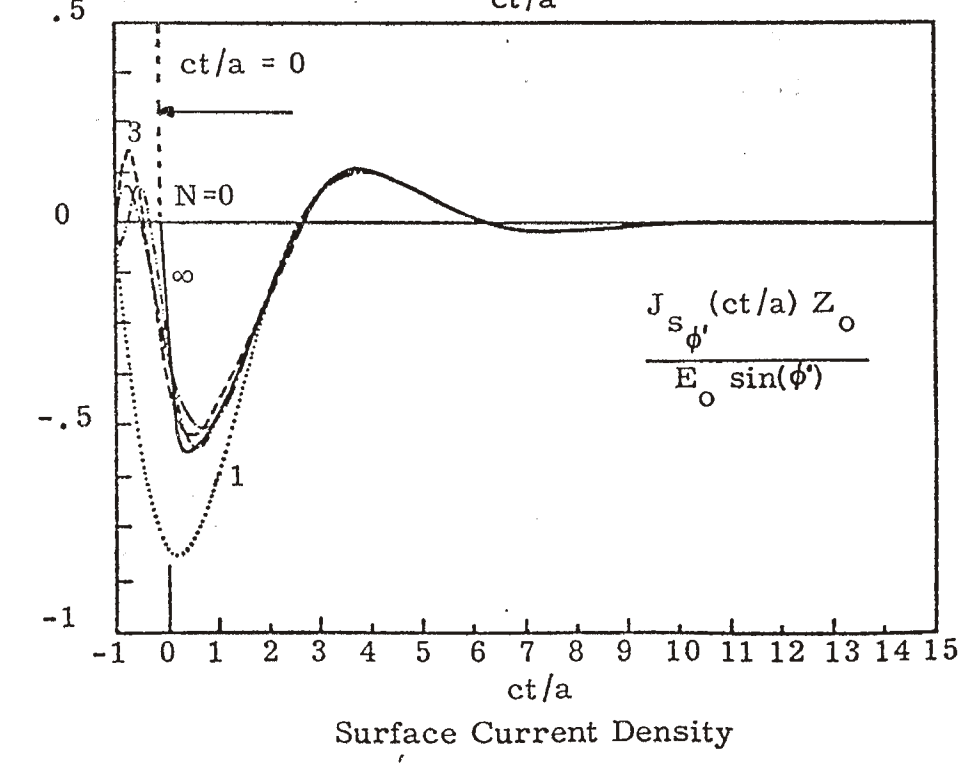

Surface Current Density

Figure 5. Step Function Response for Surface Current and Charge Densities. $\theta' = \pi/2$.

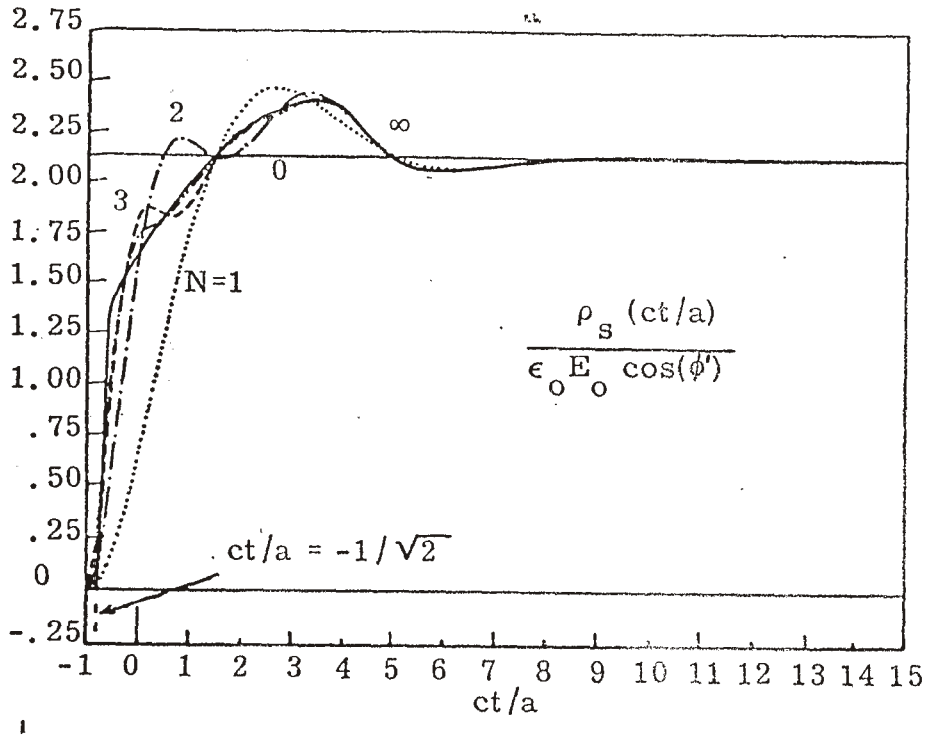

Surface Charge Density

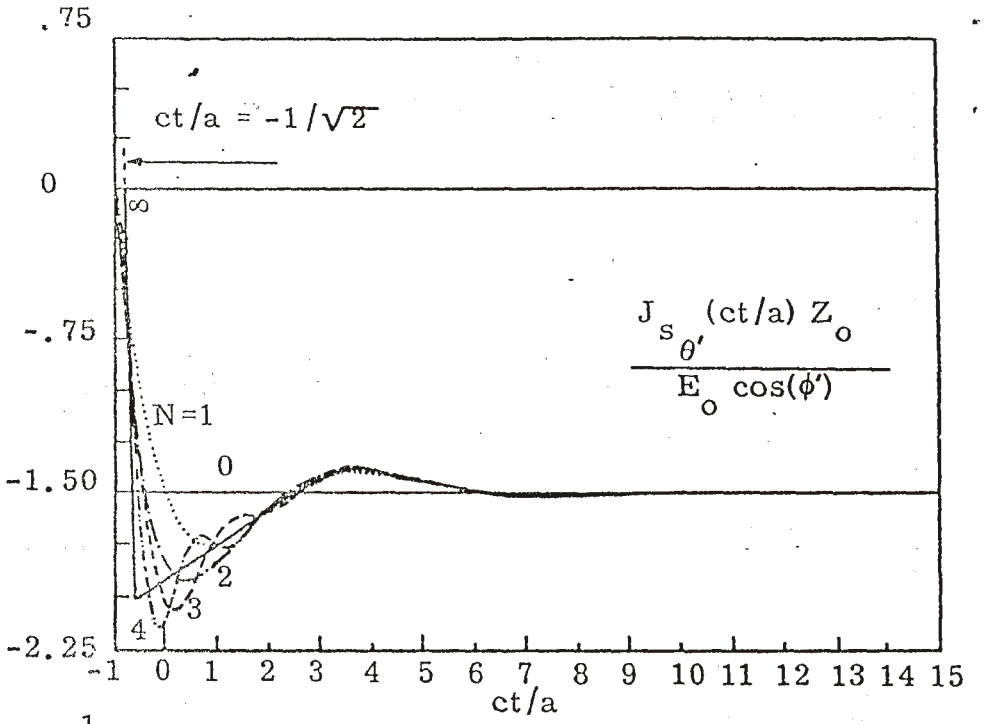

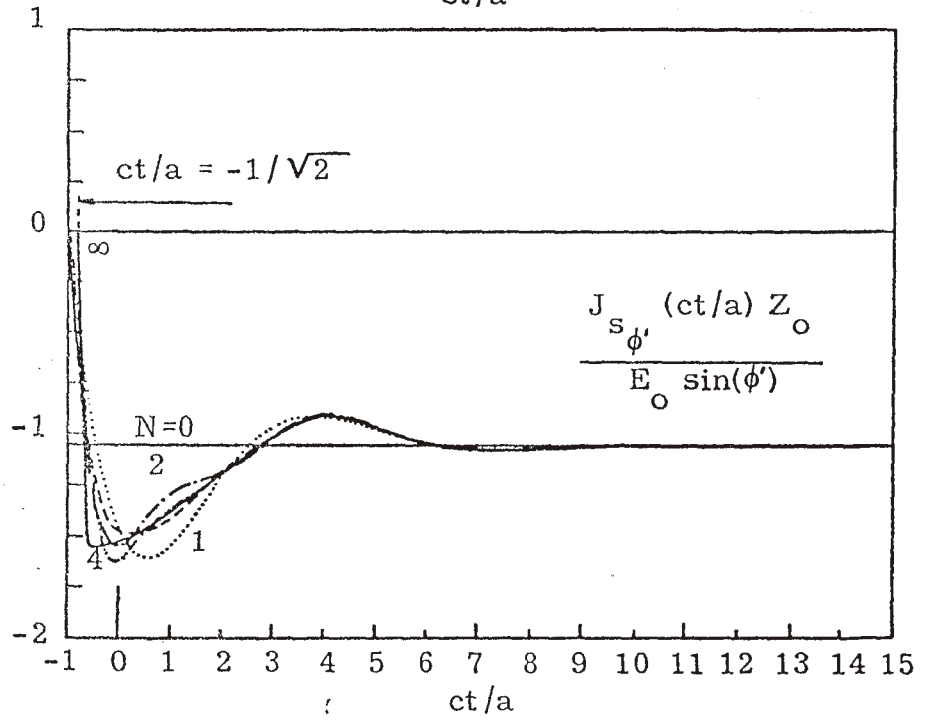

Surface Current Density

Figure 6. Step Function Response for Surface Current and Charge Densities. $\theta' = 3\pi/4$.

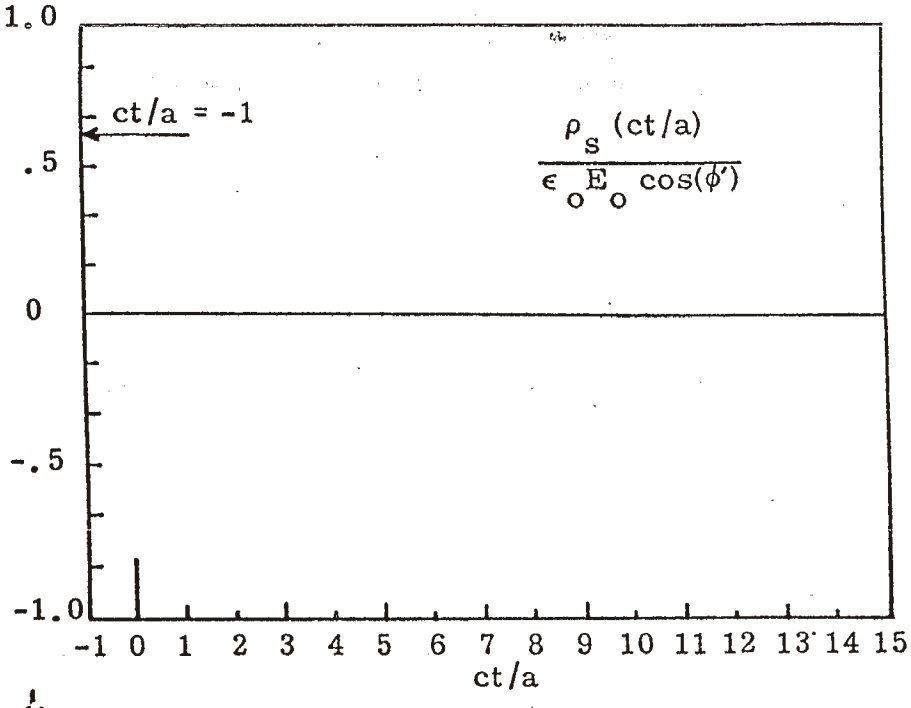

Surface Charge Density

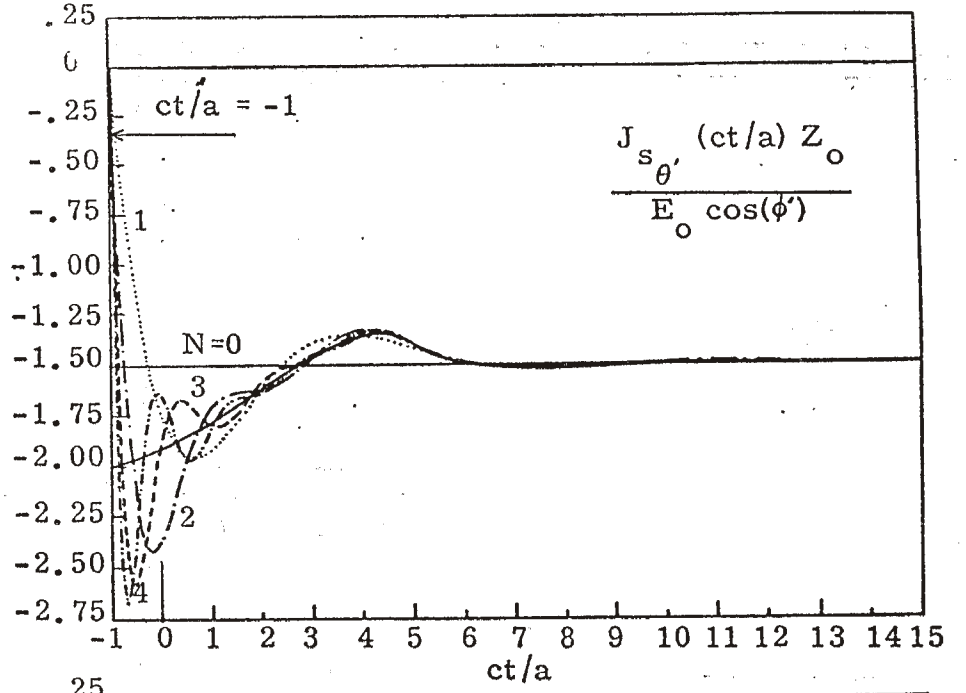

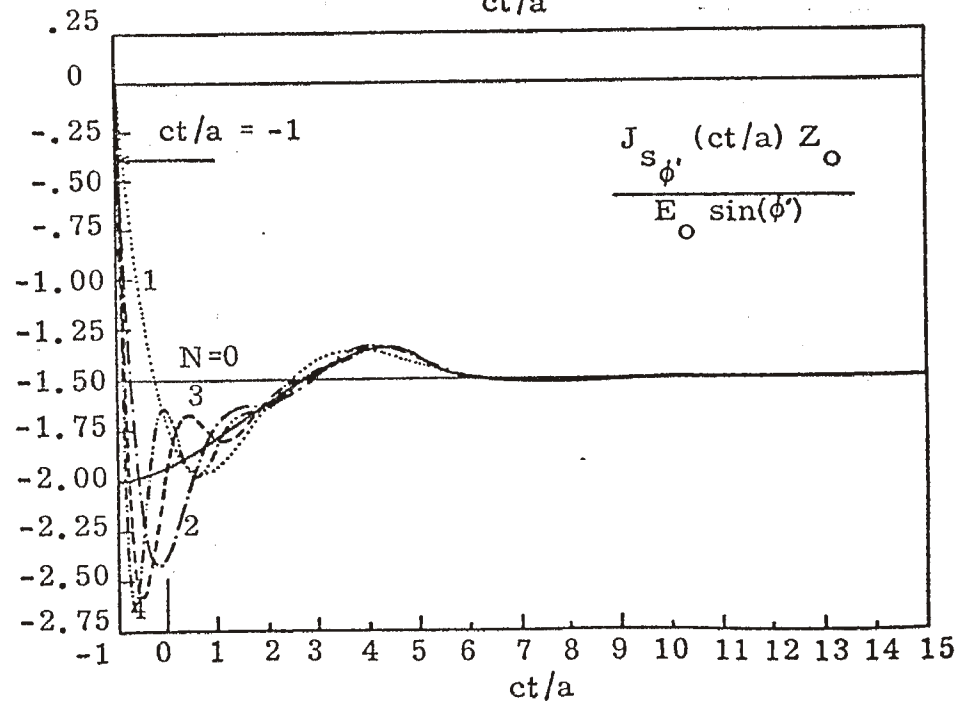

Surface Current Density

Figure 7. Step Function Response for Surface Current and Charge Densities. $\theta' = \pi$.

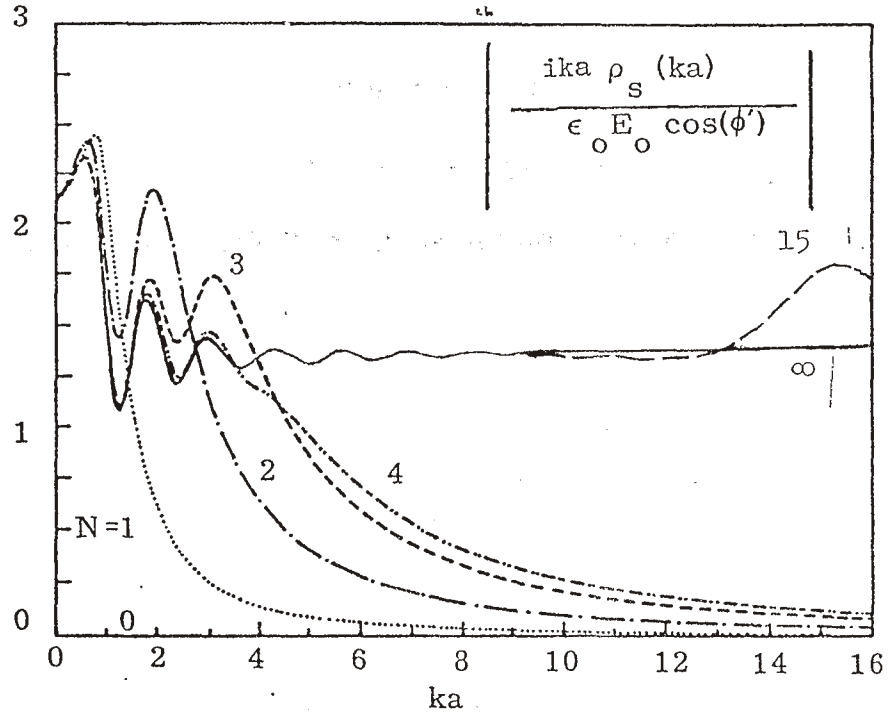

Surface Charge Density

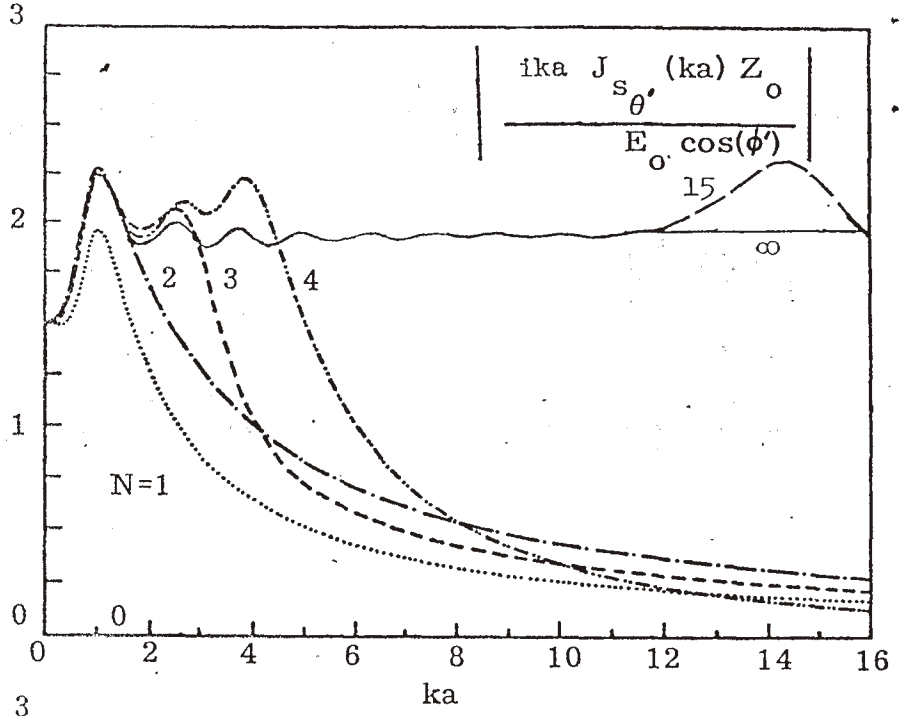

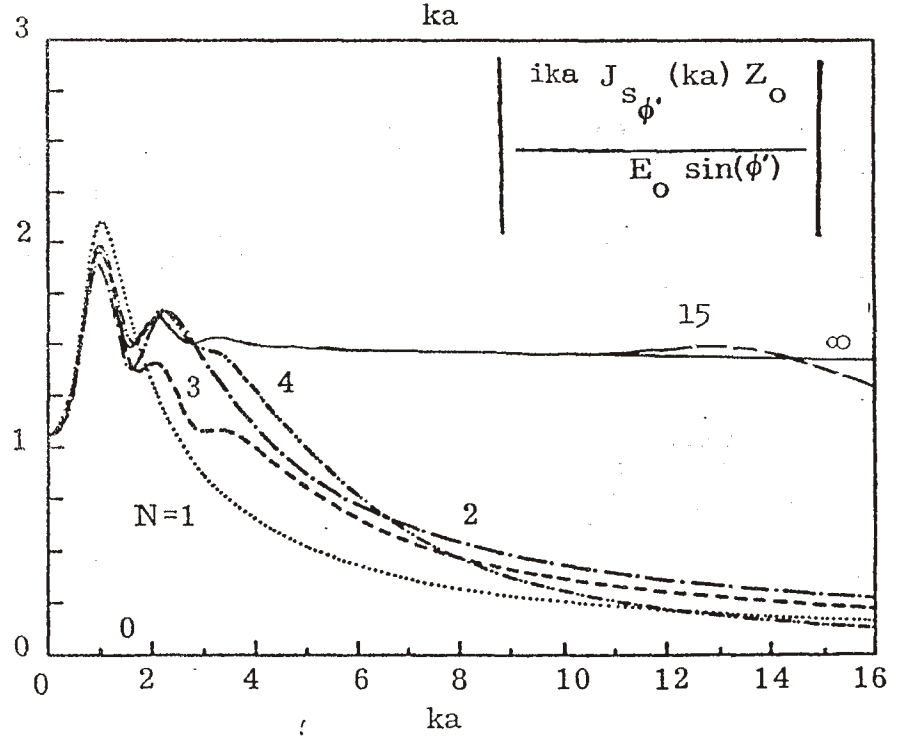

Surface Current Density

Figure 8. Step Function Response Times ika in the Frequency Domain for Surface Current and Charge Densities. $\theta' = 3\pi/4$.

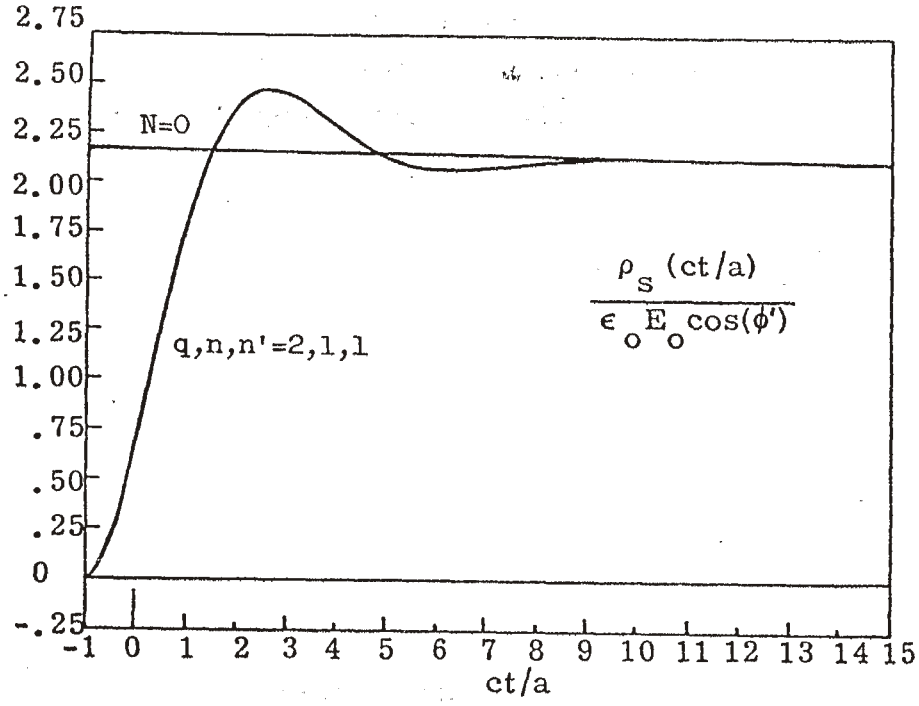

Surface Charge Density

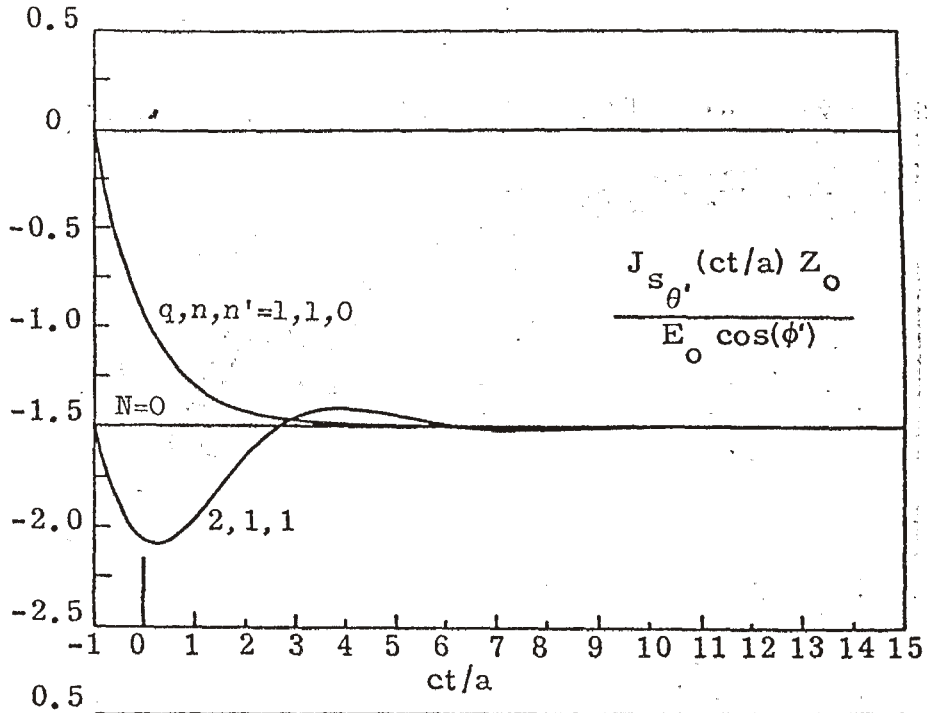

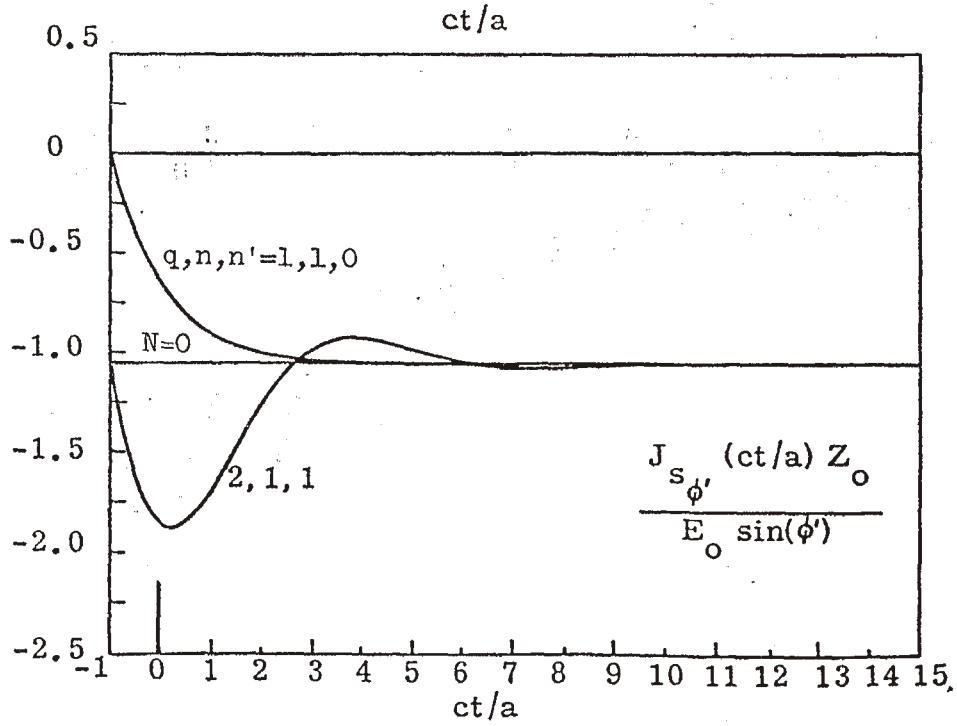

Surface Current Density

Figure 9. Surface Current and Charge Density Step Response Curves for $\theta' = 3\pi/4$. Single poles or single pole pairs are added to N=0 for n=1.

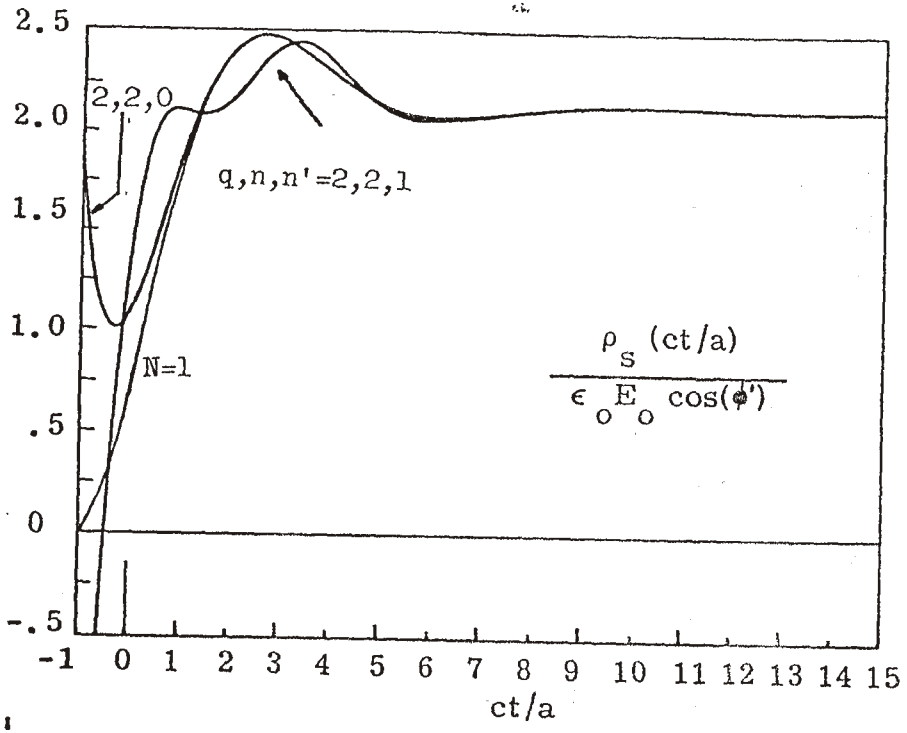

Surface Charge Density

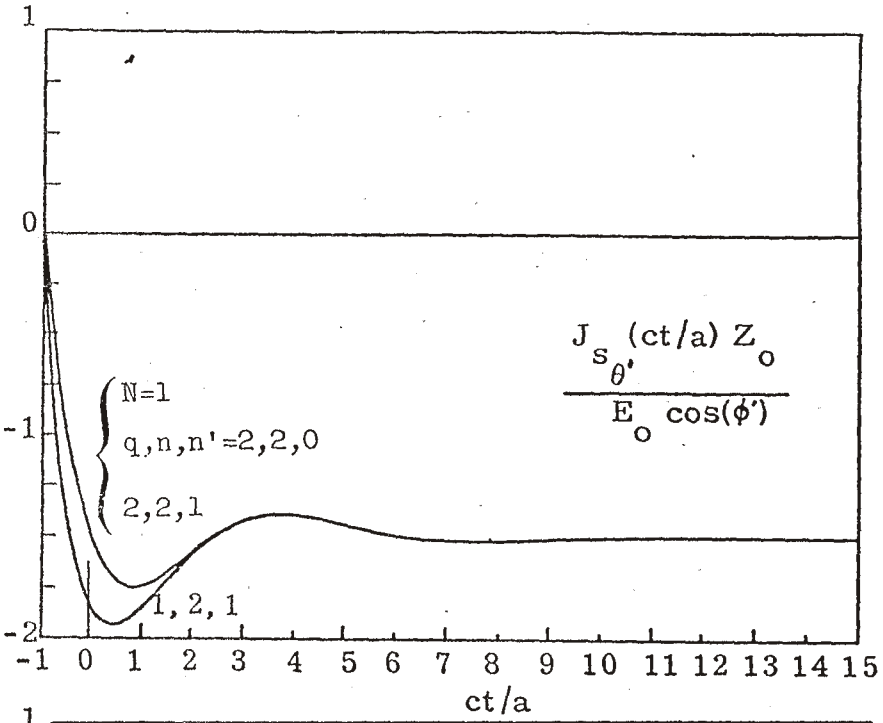

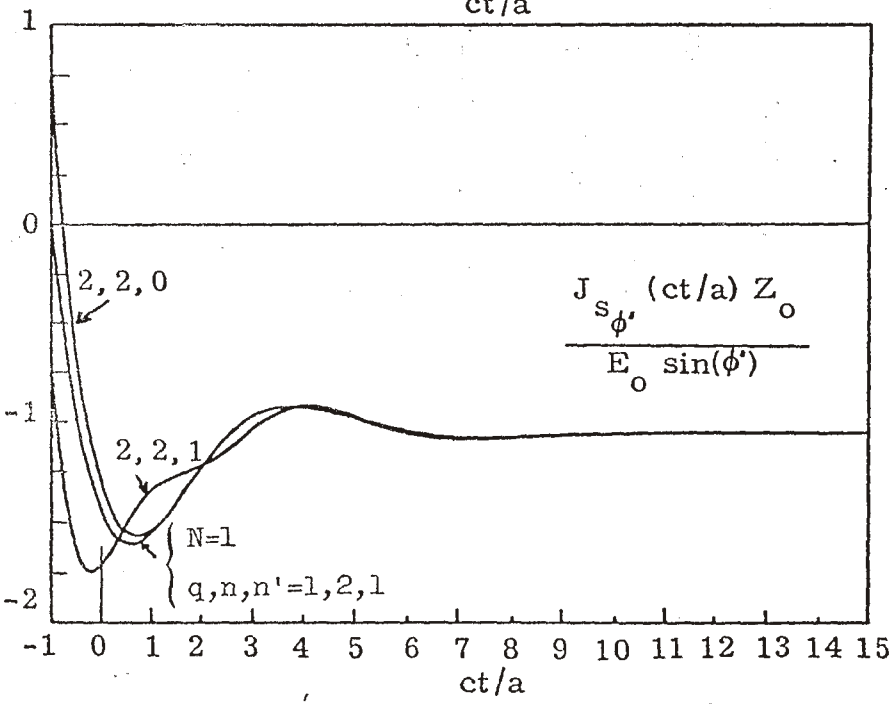

Surface Current Density

Figure 10. Surface Current and Charge Density Step Response Curves for $\theta' = 3\pi/4$. Single poles or single pole pairs are added to N=1 for n=2.

V. Conclusions

This note has taken the general equations for electromagnetic scattering by a sphere as formulated by Baum using the Singularity Expansion Method, and obtained numerical results for the induced surface currents and charges in the frequency and time domains. A comparison of these results with those obtained by the conventional frequency domain analysis with a Fourier transformation has also been made.

It can be generally said that the results of the Singularity Expansion Method compare very favorably with those of the conventional technique, provided the proper number of poles are considered. For late times, only a few poles are needed to have reasonable agreement between the two methods. For earlier times, more poles are needed for the same degree of accuracy.

The most beneficial aspect of this method, however, is that a complete description of the time dependent behavior of the spherical obstacle can be had by tabulating the pole locations, and coupling coefficients as in Table I, and by knowledge of the natural mode vectors. In the case of the spherical obstacle, these natural modes are described by the Legendre polynomials.

From the results of this study as applied to the special case of a spherical obstacle, it can generally be said that the Singularity Expansion Technique provides a new method for treating EMP interaction problems. At present, the more general aspects of this method are being studied.

References

1. Baum, C. E., "On the Singularity Expansion Method for the Solution of Electromagnetic Interaction Problems," EMP Interaction Note 88, December 1971.

2. Stratton, J. A., Electromagnetic Theory, McGraw-Hill, pp. 558, 559.

3. Marin, L., and R. W. Latham, "Analytical Properties of the Field Scattered by a Perfectly Conducting, Finite Body," EMP Interaction Note 92, January 1972.

4. Lee, S. W., and B. Leung, "The Natural Resonance Frequency of a Thin Cylinder and its Applications to EMP Studies," EMP Interaction Note 96, February 1972.

5. Tesche, F. M., "On the Singularity Expansion Method as Applied to Electromagnetic Scattering from Thin-Wires," EMP Interaction Note 102, April 1972.

6. Granzow, K., "Transient Spherical Waves," EMP Theoretical Note 24, December 1966.

7. Abramowitz and Stegun, Eds., Handbook of Mathematical Functions, AMS55, National Bureau of Standards, 1964, p. 334.

8. Van Bladel, J., Electromagnetic Fields, McGraw-Hill, p. 520.

9. Berg, L., "LEGEN, A Subroutine for the Generation of Associated Legendre Functions of the First Kind for Real Arguments Along the Cut," Mathematics Note 3, August 1969.

10. Harrington, R. F., Field Computation by Moment Methods, McMillan, 1968, pp. 272-295.

11. Martinez, J. P., "SBF, A Subroutine for the Generation of Spherical Bessel Functions with Real Arguments and Positive Integer Orders," Mathematics Note 4, October 1969.

12. Brigham, E. O., and R. E. Morrow, "The Fast Fourier Transform," IEEE Spectrum, December 1967, pp. 63-70.